

Black Phosphorous-layered Photonic Crystal Fiber based Plasmonic Biosensor for Refractometric and Urinary Tract Infection Sensing

A Project Report

Submitted in Partial Fulfilment of the Requirements for the
Awards of the Degree

of

Master of Science in Physics

Submitted by

Plakshi Gupta
23/MSCPHY/74

Under the supervision of

Dr. Ajeet Kumar
Associate Professor



Department of Applied Physics
Delhi Technological University
(Formerly Delhi College of Engineering)
Bawana Road, Delhi – 110042

June, 2025

DEPARTMENT OF APPLIED PHYSICS

DELHI TECHNOLOGICAL UNIVERSITY

(Formerly Delhi College of Engineering)

Bawana road, Delhi – 110042

CANDIDATE'S DECLARATION

I, **Plakshi Gupta** (23/MSCPHY/74), hereby certify that the work which is being presented in the thesis entitled “**Black Phosphorous layered Photonic Crystal Fiber based Plasmonic Biosensor for Refractometric and Urinary Tract Infection Sensing**” in partial fulfilment of the requirements for the Degree of **Master of Science**, submitted to the Department of Applied Physics, Delhi Technological University, is an authentic record of my own work carried out during the period from February 2024 to May 2025 under the supervision of Dr. Ajeet Kumar.

The matter presented in this thesis has not been submitted by me for the award of any other degree of this or any other university. The work has been published in SCI expanded with the following details:

Title of the Paper (I): Highly Sensitive Black Phosphorus Layered SPR-PCF Refractometric Sensor

Author names: Plakshi Gupta, Akash Khamaru and Ajeet Kumar

Name of Journal: Plasmonics, Springer (SCIE-indexed journal, IF: 3.3)

Status of the paper: Published

Date of paper communication: 7th November 2024

Date of paper acceptance: 13th December 2024

Date of paper publication: 22nd January 2025

Title of the Paper (II): Black Phosphorus-Based SPR Photonic Crystal Fiber Biosensor for Urinary Tract Infection Detection

Author names: Plakshi Gupta, Akash Khamaru and Ajeet Kumar

Name of Journal: Plasmonics, Springer (SCIE-indexed journal, IF: 3.3)

Status of the paper: Published

Date of paper communication: 18th February 2025

Date of paper acceptance: 18th March 2025

Date of paper publication: 27th March 2025

Place: Delhi

Plakshi Gupta

Date: 9th June 2025

(23/MSCPHY/74)

SUPERVISOR CERTIFICATE

I hereby certify that the Project Dissertation titled "**Black Phosphorous layered Photonic Crystal Fiber based Plasmonic Biosensor for Refractometric and Urinary Tract Infection Sensing**" which is submitted by **Plakshi Gupta**, Roll No. **23/MSCPHY/74**, Department of Applied Physics, Delhi Technological University, Delhi in partial fulfilment of the requirement for the award of the degree of **Master of Science**, is a record of the project work carried out by the student during the period from February 2024 to May 2025 under my supervision. To the best of my knowledge this work has not been submitted in part or full for any Degree or Diploma to this University or elsewhere. I, further certify that the publication and indexing information given by the student is correct.

Place: Delhi

Dr. Ajeet Kumar

Date: 9th June 2025

(Supervisor)

Abstract

This work proposes highly sensitive photonic crystal fiber based on surface plasmon resonance for sensing applications. The proposed sensors function as refractometric sensor, biosensors for detecting various diseases such as Urinary Tract infection, and cancer. All the proposed sensors are capable of detecting changes in refractive index in surroundings with an exceptional sensitivity. All the proposed fibers are simulated computationally by FEM using COMSOL Multiphysics Software. Various performance parameters were numerically analysed such as confinement loss, effective mode index, wavelength and amplitude sensitivity. With the proposed designs, high sensitivity and low confinement loss have been reported in the sensing range of RI of 1.3 to 1.4, which covers the refractive indices of most chemical and biological analytes, making it suitable for many sensing applications. The higher sensitivity magnitudes show that the proposed sensors are capable of detecting even small changes in the surrounding environment in terms of RI. Various fabrication techniques are also suggested which can be used for production of these sensors for real world applications.

Acknowledgement

I want to extend my heartfelt gratitude to my esteemed Supervisor, Dr. Ajeet Kumar, whose unwavering support, insightful guidance and invaluable mentorship has been instrumental at every stage of this research work on the applications of Surface Plasmon Resonance phenomenon in Photonic Crystal Fibers. His expert advice has been invaluable in shaping the direction and success of this work. My deepest thanks to Prof. Vinod Singh, Head, Department of Applied Physics, for providing the essential facilities and a conducive environment for our research.

I am also deeply thankful to the committee members for their critical input and suggestions, which have significantly enhanced the quality of my research work. I gratefully acknowledge Delhi Technological University for offering me the opportunity to conduct this research and for the extensive resources and support provided.

A special note of thanks to Mr. Akash Khamaru, a PhD scholar, for his constant motivation and invaluable assistance. His encouragement and help have been a great source of inspiration throughout my research journey.

Lastly, my heartfelt gratitude to my friends and family. Their unwavering love and support have been my constant source of strength and motivation throughout this journey.



Plakshi Gupta
(23/MSCPHY/74)

Table of Contents

Candidate's Declaration and Supervisor's Certificate	ii
Abstract	iv
Acknowledgement	v
Table of Contents	vi
List of Figures	viii
List of Tables	x
List of Abbreviations	xi
List of Publications	xii
CHAPTER 1 – Introduction	1-3
1.1 Aim of Thesis	
1.2 Thesis Organisation	
CHAPTER 2 – Optical Fibers	4-5
2.1 Introduction	
2.2 Types of Optical Fibers	
2.3 Special Fibers: PCFs	
CHAPTER 3 – Photonic Crystal Fibers (PCF)	6-8
3.1 Introduction	
3.2 Types of PCFs	
3.3 Applications of PCFs	
CHAPTER 4 – Surface Plasmon Resonance (SPR)	9-10
4.1 Introduction	
4.2 Biological Setup	
4.3 History of SPR Sensors	
CHAPTER 5 – Combining SPR and PCF	11-13
5.1 Types of SPR based PCFs	
5.2 Advantages of SPR based PCFs	
5.3 Disadvantages of SPR based PCFs	
CHAPTER 6 – Plasmonic Materials	14-17
6.1 Introduction	
6.2 Emerging Materials	
6.3 Black Phosphorus (BP)	
6.3.1 Fabrication of BP	

6.3.2	Advantages of BP	
CHAPTER 7 – SPR based Biosensor		18-21
7.1	Introduction	
7.2	Cancer	
7.3	Urinary Tract Infection (UTI)	
CHAPTER 8 – Numerical Analysis		22-26
8.1	Introduction	
8.2	Properties Defining a PCF	
8.3	Simulation Software	
8.3.1	COMSOL Multiphysics Software	
8.4	Numerical Analysis	
8.4.1	Finite Element Method (FEM)	
8.4.2	Finite Difference Time Domain Method	
CHAPTER 9 – Highly Sensitive Black Phosphorus–Layered SPR-PCF Refractometric Sensor		27-37
9.1	Introduction	
9.2	Structural Design	
9.3	Methodology	
9.4	Result and Discussions	
9.5	Conclusion	
CHAPTER 10 – Black Phosphorus-Based SPR Photonic Crystal Fiber Biosensor for Urinary Tract Infection Detection		38-49
10.1	Introduction	
10.2	Structural Design	
10.3	Methodology	
10.4	Fabrication Feasibility of the Proposed Design	
10.5	Result and Discussions	
10.6	Conclusion	
CHAPTER 11 – Conclusion and Future Scope		50-51
11.1	Conclusion	
11.2	Future Scope	
REFERENCES		52-56
APPENDICES		57-62

List of Figures

Fig. No.	Title of the Figure	Page No.
2.1	Phenomenon of TIR	4
2.2	Cross Sectional View of Step Index Fiber	5
3.1	Types of PCFs	7
4.1	Setup For Biosensing	9
5.1	Types of PCF Designs	11
6.1	Fabrication of BP	17
8.1	COMSOL Multiphysics Software	25
9.1	(a) Cross section of proposed D-shaped PCF SPR Sensor (b) Schematic diagram for experimental setup	29
9.2	Electric field distribution for (a) x-polarized core mode (b) y-polarized core mode (c) SPP mode (d) coupled mode (e) dispersion relation for the optimized structure at 1.38	31
9.3	Shifts in loss peak (a) with Gold layer thickness (b) with TiO ₂ layer	32
9.4	(a) Shifts in loss peak with different BP layers and (b) sensitivity variation with BP layers	33
9.5	Shifts in loss peak with different (a) small air hole radius (b) big air hole radius	33
9.6	(a) Loss Curve and (b) amplitude sensitivity for the optimized parameters without BP. (c) Loss Curve and (d) amplitude sensitivity for optimized parameters with 13 layers of BP.	35
9.7	Polynomial fitting of resonant wavelength with corresponding RI (a) Without BP (b) With BP	35
10.1	(a) Cross-sectional view of proposed D-shaped SPR PCF Biosensor (b) Experimental setup	41
10.2	(a) Core Mode (b) SPR Mode (c) SPP Mode (d) Effective mode coupling and maximum loss	44
10.3	Loss Curves for different values of RI with variation of (a) Gold Layer thickness, (b) TiO ₂ Layer Thickness	45

10.4	Loss Curves for different layers of BP when effective RI is (a) 1.335 (b) 1.371	45
10.5	Loss Curves for different values of RI with variation of (a) Size of Bigger air hole, (b) Size of Smaller air hole	46
10.6	Performance of proposed Sensor: CL (a)Without BP (c)With BP & Amplitude Sensitivity (b)Without BP (d)With BP	47
10.7	Variation in sensitivity with increase in number of BP layers	47

List of Tables

Table. No.	Title of the Table	Page No.
7.1	Refractive Indices of different types of Cancers	19
9.1	Coefficients of fitted polynomial for the curve of Resonant Wavelength vs Analyte's RI	34
9.2	Sensitivity Comparison for the proposed SPR-PCF sensor	36
10.1	Change in Wavelength and Amplitude sensitivity when BP layer is added	48
10.2	Sensitivity Comparison for the proposed SPR-PCF sensor	48

List of Abbreviations

Abbreviation	Full Form
SPR	Surface Plasmon Resonance
PCF	Photonic Crystal Fiber
SDG	Sustainable Development Goal
TB	Tuberculosis
UTI	Urinary Tract Infection
TIR	Total internal reflection
2D	Two-Dimensional
BP	Black Phosphorus
RI	Refractive Index
CL	Confinement Loss
EMA	Effective Mode Area
PDE	Partial Differential Equation
FEM	Finite Element Method
FDTD	Finite Difference Time Domain
SMF	Single Mode Fiber
OSA	Optical spectrum analyzer
SPP	Surface Plasmon Polariton
IR	Infrared

List of Publications

- **Publications Related to Thesis**

- **Journal Publications**

1. **Plakshi Gupta**, Akash Khamaru, Ajeet Kumar, “Highly Sensitive Black Phosphorus Layered SPR-PCF Refractometric Sensor” **(Published in Plasmonics, Springer on 21st January 2025) (SCIE-indexed journal, IF: 3.3)-** <https://doi.org/10.1007/s11468-024-02723-5>
2. **Plakshi Gupta**, Akash Khamaru, Ajeet Kumar, “Black Phosphorus-Based SPR Photonic Crystal Fiber Biosensor for Urinary Tract Infection Detection” **(Published in Plasmonics, Springer on 26th March 2025) (SCIE-indexed journal, IF: 3.3)-** <https://doi.org/10.1007/s11468-025-02911-x>

- **Publications Out of The Thesis**

- **Conference Publications**

1. Arhee Bhuyan, **Plakshi Gupta**, Akash Khamaru, Ajeet Kumar, “Design and Analysis of Black Phosphorus layered SPR-PCF Biosensor for Detection of Cancerous Cells”, PHOTONICS 2024, 12-15th December 2024, IIT Kharagpur, West Bengal, India **(poster presented and full-length paper communicated)**

1

Introduction

Surface Plasmon Resonance (SPR) integrated with Photonic Crystal Fibers (PCFs) is an innovative approach in photonic sensing technologies. This report focuses on the theoretical design and simulation of SPR-PCFs for enhanced optical sensing capabilities. Using COMSOL Multiphysics software, we designed our proposed PCFs with favourable material compositions and analysed the interaction of surface plasmons with guided light modes in PCFs, emphasizing sensitivity and spectral response. Our findings demonstrate improved performance in biosensing and chemical detection applications compared to conventional PCFs.

SPR is a phenomenon that occurs at the surfaces of the metals (like gold, silver), whenever electrons interact with the light beam that strikes the surface at a specific angle [1]. The interaction is sensitive to the changes in the nearby environment, or simply the changes in refractive index (RI). On comparing with the traditional sensing methods, the sensing technology adopting SPR technique has advantages of real time analysis; it is much more sensitive to the changes in surroundings, and is label free. Therefore, SPR sensing approach has proved as remarkable detection technique due to higher sensitivity and a vast number of applications like biosensing, antibody interaction, clinical trials, food quality analysis, and gas detection.

Biosensors are tools used to analyze biological substances. They have two main parts: a biological element (like tissue, microorganisms, enzymes, or antibodies) and a physical-chemical detector. When the target substance (analyte) interacts with the biological element, it causes a change that the detector can sense. This detector then converts the change into an electronic signal that tells you how much of the target substance is present.

PCFs are upgraded version of a regular optical fiber but has tiny air holes running along its length. These air holes help control how light moves through the fiber, making it possible to manipulate light more precisely than with traditional fibers [2]. One can

design these fibers in different shapes and sizes to achieve specific light-handling properties.

In current scenario, numerous SPR PCF sensors have been proposed altering the prism-based technique [3]. There are many types of SPR-PCFs designs using metal-coated holes [4], U-grooved [5] etc. are already proposed in previous literatures. But they inherit some disadvantages like, fabrication complexity, difficulty in deposition of metals in holes [6], etc. Several D-shaped PCFs which are flat from the top are also being reported. The top portion of PCF with air holes is polished. This provides larger area for interaction between core-guided light and surface plasmons, effectively improving the overall sensitivity.

Sustainable development goal (SDG) 3.3 focuses on the solutions of epidemics like Cancer, AIDS, hepatitis, Tuberculosis (TB), Urinary Tract Infection (UTI) and others. An effective early disease detection method is essential to obtain this objective. SPR influenced biosensors are now being widely recognized as an effective method for detecting the biomolecular interactions in real time, without any need of labelling.

1.1. Aim of Thesis

Primary objective of this thesis work is as follows:

- To design surface plasmon based PCF sensor for different applications.
- To study the effect of different types of 2-dimensional materials (e.g., black phosphorus (BP), graphene, MoS₂) used as plasmonic materials for increasing sensitivity of the sensors.
- To simulate the optical properties of the designed sensors using the Finite Element Method (FEM) in COMSOL Multiphysics Software.
- To analyse the performance metrics such as confinement loss (CL), sensitivity, figure of merit etc. under different conditions.
- To optimize the designed fiber for achieving high sensitivity and low loss, by tuning the structural parameters.
- To explore sensor's capability in sensing any specific disease (e.g., cancer, UTI) based on RI variations of analytes.

1.2. Thesis Organisation

The present work is organised into 12 chapters:

- Chapter 1 contains the introduction of all the topics of the thesis such as SPR, PCF, etc. It also contains the aim of thesis and thesis organization.
- Chapter 2 is aimed at exploring optical fibers and its types.
- Chapter 3 explores PCFs in detail, along with its types.
- Chapter 4 draws the attention towards the SPR in detail.
- Chapter 5 combines SPR and PCF and contains the advantages of doing so.
- Chapter 6 explains about the plasmonic materials along with the detailed explanation on BP material.
- Chapter 7 contains the explanation about Biosensors and various diseases explored to create one.
- Chapter 8 is aimed to explore the optical properties, simulation software and numerical methods used to carry out the research.
- Chapter 9 contains the first main project on designing a refractometric sensor with BP for offering higher sensitivity.
- Chapter 10 contains the second main project on designing a biosensor to detect UTI with great precision.
- Chapter 11 contains the third main project of designing a biosensor to detect cancer with high accuracy.
- Chapter 12 draws out conclusion and future scope.

2

Optical Fibers

2.1. Introduction

Optical Fibers are a hollow structured waveguide which are made up of the dielectric material where a light can travel from one place to another or the information can travel from one place to another using the total internal reflection phenomenon (TIR). In TIR, the light striking the interface of two different mediums is not refracted back into second medium but gets reflected back into the first medium, as shown in Fig 2.1. There are two necessary conditions for TIR to occur:

- i) The light must travel from a medium of higher RI (denser medium) to a medium of lower RI (rarer medium).
- ii) The angle of incidence on the interface of the media must be greater than the critical angle (θ_c) at the interface.

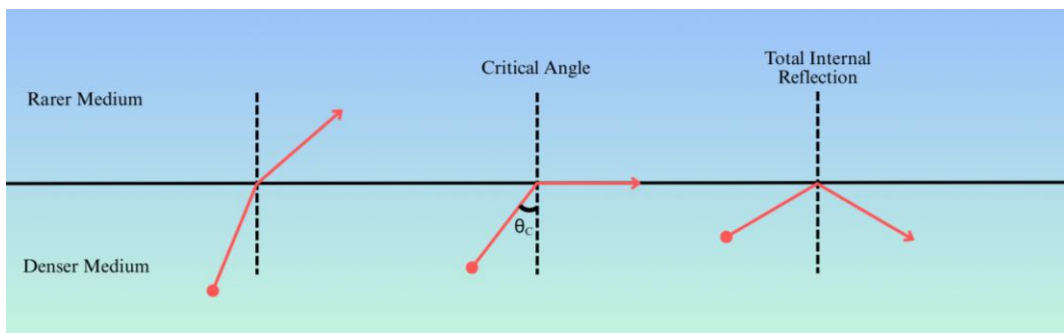


Fig 2.1. Phenomenon of TIR

An optical fiber comprises of two main parts (Fig 2.2):

1. **Core** - It is a higher RI (n_1) region in the optical fiber which is mostly made up of silica. The light guidance takes place here with the help of the TIR.
2. **Cladding** - It is the lower RI (n_2) region surrounding the core region in the optical fiber. It is made up of any optically transparent material having lower RI than that of core.

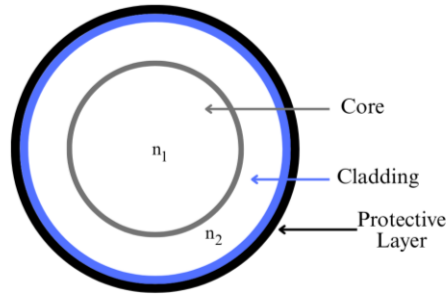


Fig 2.2. Cross Sectional View of Step Index Fiber

2.2. Types of Optical Fibers

Optical fibers can be classified on the basis of the structural design. They are mainly classified as:

a. Single-mode Fiber

The core diameter in such fibers is reduced to a limit such that they allow only fundamental mode to propagate through them. These fibers have the core diameter of few wavelengths as compared to the wavelength of light propagating into the fiber. These fibers do not exhibit modal dispersion hence are more compatible for long range communications.

b. Multi-mode Fiber

The fibers which allow multiple modes of light to propagate through them are known as multimode fibers. The diameter of core in multimode fibers is larger than wavelength of light propagating through them. The number of modes that can propagate through them is directly proportional to the diameter of core.

2.3. Special Fibers: PCFs

PCFs use photonic crystals for the cladding and core. The core region is high index region and cladding consists of air holes arranged in a certain manner which reduces the RI of cladding region. PCFs are more efficient than conventional fibers as the RI of the core and cladding region can be changed easily either by changing the arrangement or shape of air holes in the cladding region or by altering size of air holes in the cladding region. Losses in PCFs are also low as compared to conventional fibers.

3

Photonic Crystal Fibers

3.1. Introduction

PCFs are special types of optical fibers which have tiny air holes running along its length. These air holes control how the light moves throughout the fiber. It is possible to manipulate the light propagation more precisely with PCFs than with traditional fibers. PCFs have the advantages of high birefringence, higher nonlinearity, and flexible structural design. These properties give rise to a large number of applications like terahertz communication [7], terahertz-based sensors [8], RI sensors [9], pressure sensors [10], supercontinuum generation, magnetic field sensor [11], high-power fiber lasers, etc. PCFs are currently being produced in a large number of laboratories by using different techniques like stacking of capillaries and rods extrusion, sol-gel casting, and drilling. Materials such as silica, fluoride glasses, polymers, and chalcogenide glasses are being used for the fabrication of PCFs [2]. PCF-based SPR sensors arise as types of sensors that are used to detect tiny amounts of substances in various domains such as biology, environment, and medicine. Looking at its advantages, such as smaller size, single mode propagation, effortless light launching, and ability to control evanescent field penetration, have made it a promising candidate for sensing. The light enters and travels through the core of the PCF and as the light strikes the plasmonic material (like silver, gold), it causes electrons in the metals to oscillate. A strong interaction happens when light and electron oscillations match up and the phenomena is known as resonance. If the environment around the fiber changes, or RI of the analyte changes, the resonance condition shifts. This shift changes the incident light's wavelength, which a PCF-SPR sensor can detect.

3.2. Types of PCFs

1. Index Guiding PCF:

Light, by TIR is centred between core and air gaps (known as cladding). The solid core of controlling PCF exhibit air gaps (Fig. 3.1(a)), which is encompassed by unadulterated silica cladding with RI of 1.462.

2. Photonic Band gap Fiber:

When the core part in the air holes array is replaced by a bigger hole of much bigger diameter in comparison with the surrounding holes, as shown in Fig. 3.1(b).

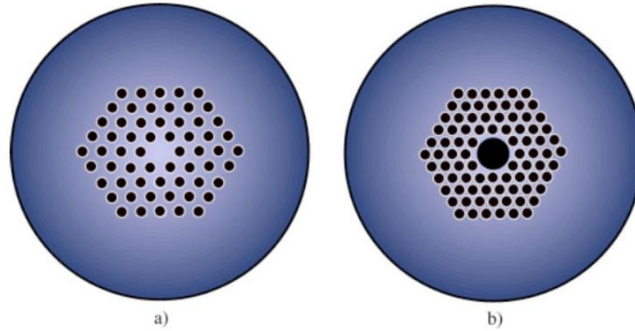


Fig.3.1. Types of PCFs (a) Index Guiding PCF
(b) Photonic Band Gap Fiber. Ref. at [12]

3.3. Applications of PCFs:

PCFs are a specialized type of optical fiber that uses periodic variations in the RI to control the propagation of light. Their unique properties make them valuable in various applications across different fields:

1. **Telecommunications:** PCFs allows improved data transmission due to their ability to guide line over long distances with high-bandwidth and low transmission loss.
2. **Sensing and Measurements:** PCFs can be altered to interact with a particular wavelength or wavelength range, which makes them a good candidate for various chemical and gas sensing applications. They're used in industries like environmental monitoring, healthcare (for medical diagnostics), and security (for detecting hazardous materials).
3. **Nonlinear Optics:** The design of PCFs can help in achieving non linearity and thus can be used in nonlinear optics to make lasers and optoelectronic devices. Nonlinearity offered by the PCFs can help in invoking certain phenomenon like Raman Scattering, four-wave mixing which can help in laser optics and SC generation.
4. **Light generation and Manipulation:** White light generation can also be achieved by employing PCFs. Generation of light over large spectrum of

wavelengths can be achieved. This is used in diverse applications like medical imaging, early cancer detection, spectroscopy and optical coherence tomography for high resolution imaging.

5. **Quantum Optics:** Due to their ability to control the flow of light and interaction of photons, PCFs can be explored in quantum optics also.
6. **High Power Laser delivery:** They are capable of guiding high-power laser light without damage due to their design, making them suitable for applications in laser machining, surgery, and defence.

4

Surface Plasmon Resonance

4.1. Introduction

Surface plasmon resonance (SPR) is a phenomenon that occurs at the metal surfaces (mostly gold and silver) when any incident light beam hits the surface at a particular angle. Depending on the thickness of the molecular layer at metal surfaces, the SPR phenomenon results in a reducing the intensity of the reflected light. Biomedical applications take an advantage of SPR by using RI of the medium next to the metal surface, making it possible to measure accurately, the adsorption of molecules on the metal surfaces and their final interactions with any specific ligands/proteins.

4.2. Biological Setup

When using the SPR Technique for Biosensing, the following experimental Setup is observed, shown in Fig 4.1:

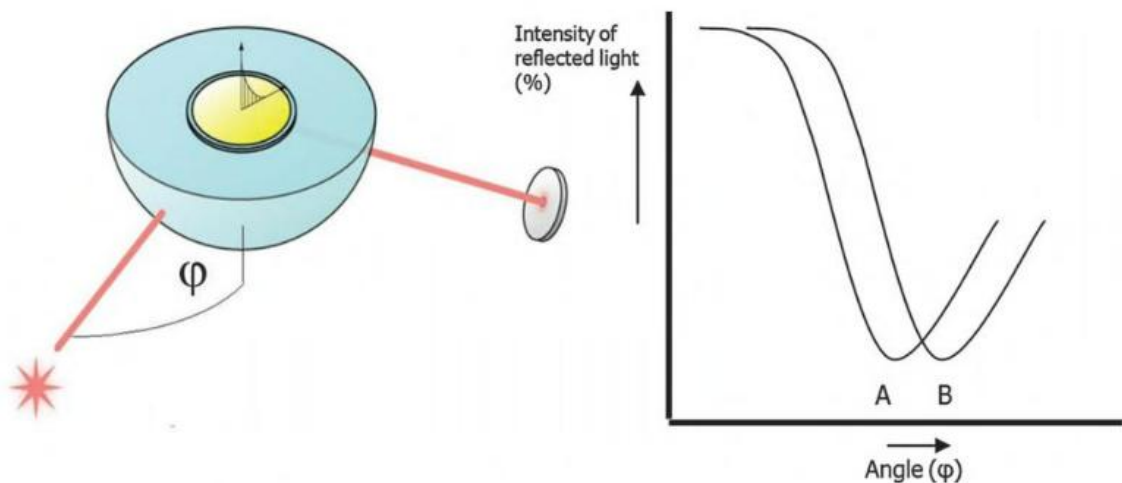


Fig.4.1. Setup For Biosensing

[Image by IBIS Technologies via <https://www.ibis-spr.nl/product/optics/>]

Imagine one have a setup where light passes through a prism and hits a sensor chip with a thin layer of metal (Gold) on it. This metal layer usually acts like a mirror, reflecting the light back. When you change the angle at which the light hits the metal and

measure how much light is reflected, you'll notice that the reflected light intensity drops to a minimum at a specific angle. This happens because at that particular angle, the light excites surface plasmons on the metal. Initially, nothing happens at the sensor, and we measure a baseline with the dip at the SPR angle (A). When we inject the sample, biomolecules stick to the surface, causing a change in the RI and shifting the SPR angle to a new position (B). This is called association. When the sample with the analyte is replaced with a buffer solution, the analyte starts to detach from the ligand, which is called dissociation. We can watch this adsorption and desorption process in real time and figure out how much of the biomolecules have attached.

4.3. History of SPR Sensors

Surface plasmons are waves created by the movement of free electrons in the metal when they interact with the light. This interaction reduces the amount of light reflected, creating a dip in the intensity.

Surface plasmons (SPs) were initially introduced by Ritchie, in 1950s [13]. By applying the theory of SPs, SPR configuration with prism coupling was studied by Otto where the prism and plasmonic materials were separated by a dielectric medium. The setup's configuration was then updated by the Kretschmann where prism and plasmonic material were placed in a direct contact. The latter configuration was used for creating surface plasmon waves, by matching the frequency of incident light and surface electrons (i.e. free electrons in metals). In 1980s, these methods were used to demonstrate SPR sensor for biological and chemical sensing. The prism based Kretschmann setup is now being widely used for SPR sensors, in which prism is coated with the plasmonic material. The deviation in the RI changes the propagation constant of surface plasmon mode. This results in variation in coupling conditions. But the prism based SPR sensor requires a bulky configuration with optical and mechanical components and also not cost friendly. As a result, the discussed configurations are not suitable for field-based applications [1]. These limitations of prism based SPRs gave rise to the optical fiber based SPR sensors in 1990s. The fiber based SPR sensors were being used to provide a wider operating range and better resolution. But the major disadvantage of traditional PCF SPR sensors is that they require the direct incidence of light at a narrow angle. To overcome these problems, PCFs were introduced in 2000s for employing them for SPR based detection [2].

5

Combining SPR and PCF

5.1. Introduction

SPR-PCF sensor is a special type of sensor used to detect tiny amounts of different substances (called analytes) in various fields like biology, environment, and medicine. It combines two advanced technologies: PCF and SPR. Light enters and moves through the core of the PCF. The light hits a metal layer (like gold) inside the fiber, causing the electrons in the metal to oscillate (move back and forth). When the light and electron oscillations match up just right, a strong interaction happens, called resonance. This interaction causes a noticeable dip in the light that passes through. If the substance around the fiber changes (like a new chemical or biological sample being present), the resonance condition shifts. This shift changes the light's behavior, which the sensor detects.

5.2. Types of SPR based PCFs

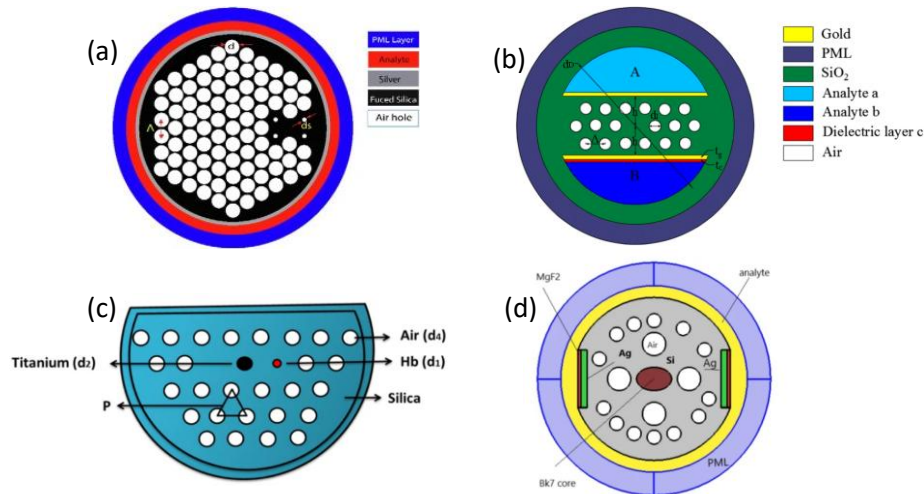


Fig 5.1. Types of PCF Designs (a) External Metal Layer Coating (b) Internal Metal Coating (c) D-shaped PCF (d) Side Polished Fiber
Ref. at [14,15,16,17]

1. **External Metal Layer Coating:** In this model, Fig 5(a), a thin layer of plasmonic material (like gold or silver) is coated on the external surface of PCF. It simplifies

fabrication as it avoids complex internal deposition processes and enhances sensor performance by facilitating interaction between the core mode and the surface plasmon wave [14].

2. **Internal Metal Coating:** In this model, Fig 5(b), the plasmonic metal layer is deposited inside the selective microscopic air holes of the PCF. This method is technically challenging due to the precision required in coating the internal surfaces uniformly [15].
3. **D-shaped PCF:** This model, Fig 5(d), involves polishing the top portion of the PCF with air holes to form a D-shape. The flat surface is then coated with a plasmonic metal layer. The D-shaped structure allows for a larger interaction area between the core-guided light and the surface plasmons, improving sensitivity [16].
4. **Side Polished Fiber:** In this model, Fig 5(c), the PCF is polished from one side to bring the plasmonic metal closer to the core, thereby enhancing the interaction between the core mode and the surface plasmon mode. Polishing depth can be controlled to optimize the sensor's performance [17].

5.3. Advantages of SPR based PCFs

1. **High Sensitivity:** PCF SPR sensors offer high sensitivity due to the strong interaction of light with plasmonic waves.
2. **Design Flexibility:** The ability to tailor the PCF structure allows for optimizing sensor performance for specific applications.
3. **Broad Application Range:** Applications in biosensing, biomedical imaging, environmental monitoring, and chemical sensing are highlighted.
4. **Enhanced Light Confinement:** The microstructured geometry of PCFs ensures better light confinement in the core and around the plasmonic interface, increasing the interaction between light and the analyte, which improves sensitivity.
5. **Enhanced Performance with 2D Materials:** Incorporating materials like graphene and MoS₂ can improve biomolecule adsorption and sensor sensitivity.

6. **Compact and Lightweight Design:** SPR-PCF sensors are compact, making them ideal for portable sensing devices. The small size and low weight facilitate integration into miniaturized systems for field applications.
7. **Real-Time Monitoring:** SPR-PCFs enable real-time and continuous monitoring, which is crucial for applications in medical diagnostics, industrial processes, and environmental sensing
8. **High Resolution:** SPR-PCFs can detect minute changes in RI due to their high resolution, making them suitable for detecting trace amounts of analytes.

5.4. Limitations of SPR based PCFs

1. **Complex Fabrication:** The manufacturing process is more complex compared to traditional fibers, especially for structures requiring precise metal layer deposition. Using advanced fabrication techniques like sol gel method, stack and draw method helps in reducing the error in prototyping of the complex fabrications.
2. **Material Limitations:** Issues such as poor biomolecule adsorption with traditional plasmonic metals (e.g., gold) and susceptibility to oxidation (e.g., silver). Applying metal coatings to enhance biomolecule affinity and to prevent metal degradation reduces material's limitations.
3. **Resonance Peak Broadening:** The use of gold can result in a broad resonance peak, reducing detection accuracy.
4. **Limited Metal Choices:** Though gold and silver are the most commonly used metals for SPR, alternatives like aluminium or copper are less efficient for plasmonic applications, limiting material flexibility. Researching into the emerging plasmonic materials might offer tunability and stable options for sensing.

6

Plasmonic Materials

6.1. Introduction

Surface plasmon polaritons (SPPs), are electromagnetic excitations of free electron densities at the intersection of a metal and dielectric. SPP excitation is thereby, enhanced due to the presence of large electron densities, which are provided by the metallic thin films, also known as plasmonic materials.

The selection of plasmonic material is one of the most important parts of designing an SPR-PCF sensor. The best selection of plasmonic metal is, which ensures enriched free electrons in the momentary field. Plasmonic materials like gold, silver, TiO_2 are being most commonly used.

Gold, as a plasmonic material, has advantages like it is a supreme compatible metal against corrosion and oxidation, superior optical reactions and has a very good chemical fixity. Gold (Au) is considered to be one of the best plasmonic materials due to its lower corrosion and oxidation tendency. It is free from inter-band transition loss and also shows a sharp and narrow resonance peak.

Silver is chosen as a plasmonic material because of the excellent chemical properties. It produces a sharper SPR spectrum, it is very reactive and often requires a protective overlayer. Due to its properties like low optical damping and no interstate transitions, it is a good plasmonic material. Silver has a sharp resonance peak which achieves a high detection accuracy. But, silver also suffers greatly from oxidation.

Aluminium shows the plasmonic resonance in the ultraviolet region, which makes it suitable for near infrared (IR) biosensing. Its high plasma frequency makes it more attractive for the integrated photonic devices. Its main drawback is that it forms an oxide layer which might hinder the plasmon excitation.

Copper shows the plasmonic behaviour same as that of gold and silver in the visible region, but its oxidation and corrosion occurs rapidly. To overcome this, protective metal

coatings are used to increase the stability and to prevent degradation, making copper a useful material in cost sensitive applications.

Thin TiO_2 layer is used to provide an adhesion between gold and the fiber surface. It tunes the operating wavelength of the sensor near to the IR region as the biosensor works well in this region. Adding a layer also supports excitation of plasmons between Au and dielectric interface causing an increase in the evanescent field which further increases the interaction between plasmon polariton with its surrounding medium i.e. analyte. Due to this, gold has been found to be less prone to biomolecule adsorption, potentially leading to degradation in the detection limit.

6.2. Emerging Materials

Recently, germanene, phosphorene, silicene and BP are being reported to possess very good plasmonic properties in IR and terahertz frequencies. So, in coming years, these materials may be adopted for developing potentially more sensitive biosensor implementations. Silicene is a hexagonal honeycomb 2D allotrope of silicon [18]. Germanene, just like silicene, is also a 2D honeycomb-structured, small-band-gap material with higher lifetime of plasmonic modes [19]. An important characteristic in phosphorene for plasmonic applications is the tunability of its band structure making it very useful in anisotropic plasmonic applications [20]. BP possesses a zigzagged-honeycomb structure and also produces anisotropic plasmonic response as well.

6.3. Black Phosphorus (BP)

BP is a new type of 2-D plasmonic material that is attracting the attention of researchers due to its electrical and optical properties which includes direct band gap, small work function, better binding of molecules on the surface of sensors, and high charge carrier mobility [21]. Direct band gap makes BP to interact with light at a specific wavelength which then, enhances the sensitivity of sensor. Small work function allows BP to transfer electrons between the surrounding environment and BP layers. Higher charge carrier mobility makes the sensor to transmit signals fast and efficient which results in the rapid response and higher sensitivity. Its ability to bind molecules tightly on the surface allows it to be used in biological and chemical sensing. So, BP enhances

the sensor's ability by providing molecules (like proteins, DNA, or chemical analytes) an active site to attach to. The application of BP in SPR sensors includes better biomolecule detection, environment monitoring, clinical applications, and it helps in the prevention of oxidation of plasmonic layers. These are some of the reasons that led the attraction of researchers towards BP, K. Tong, J. Wang, et al in [22] proposed an ultrashort side polished structure, with BP layers, and has the dynamic sensitivity of 8200 nm/RIU, for different values of RI starting from 1.320 to 1.375.

6.3.1. Fabrication of BP

BP is integrated into the SPR sensors by adding multiple thin layers of 0.53 nm thickness each on the surface. The layering of BP can be done through various techniques like Mechanical Peeling, Liquid Peeling, and Pulse layer Precipitation [22,23]. Mechanical peeling involves physically peeling a thin layer of BP using special tools from a larger piece. It is the most commonly used method, as it does not require complex equipment and is cost-efficient. On the other hand, the liquid peeling technique involves placing the bulk piece in a liquid and then subjecting it to ultrasound waves, which produce a large number of thin BP layers. Similarly, pulsed laser precipitation technique involves firing of powerful laser at the bulk material. This method allows to control the size and thickness of the layer.

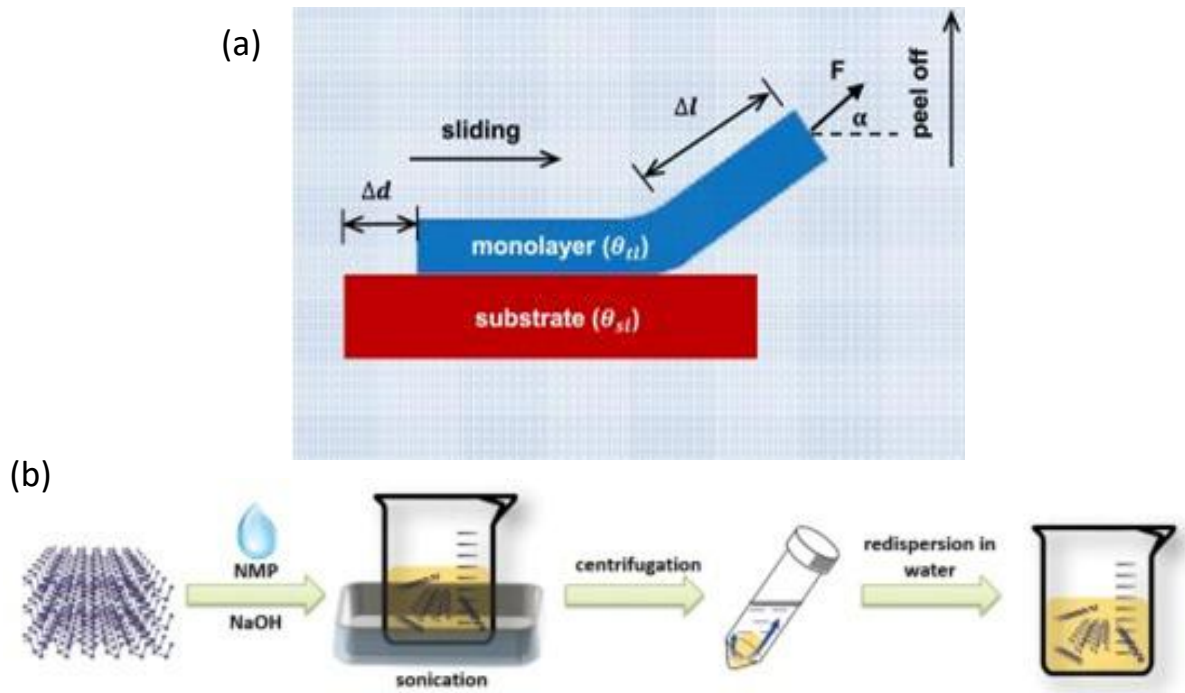


Fig 6.1. Fabrication of BP (a) Mechanical Peeling (b) Liquid Peeling. Ref. at [24]

6.3.2. Advantages of BP

1. **Biomolecular Detection:** Improved sensitivity allows for the detection of biomolecules at very low concentrations, useful in medical diagnostics.
2. **Environmental Monitoring:** Detection of pollutants and hazardous chemicals with high precision.
3. **Clinical Applications:** Real-time monitoring of biological interactions, beneficial for disease diagnosis and management.
4. Phosphorene helps in **prevention of oxidation** of the silver layer when used as a plasmonic active metal [17].

SPR based Biosensors

7.1. Introduction

Biosensors have emerged as a powerful tool in disease diagnostics due to the ability of providing fast, accurate, and non-invasive detection of diseases. The integration of SPR with biosensors has enhanced their sensitivity, and made them highly effective for detecting different diseases. This section will focus on two significant diseases where biosensors can play a crucial role: Cancer and Urinary Tract Infection(UTI).

Biosensors are the devices that combine biological recognisable elements with a physical transducer to detect the specific analytes. Diseases such as Cancer and UTIs demand early and accurate detection methods due to their impact on public health. SPR-based PCF biosensors, due to their label free and real time detection capabilities, are being widely researched for these applications. The primary focus of research is on designing biosensors with high sensitivity, specificity, and limits to detect biomarkers associated with the diseases. These biosensors offer the ability to revolutionize the diagnostics, enabling the early detection and improved patient rates.

7.2. Cancer

The human body is composed of millions of microscopic cells, and each cell functions as a different organism. Every cell works together with every other cell to form tissues and hence organs in the body. They begin to regenerate when a damaged or dead cell is found. When the process of cellular replication occurs unregularly, cancer is developed. Every cell has a nucleus which contains chromosomes, whereas these chromosomes are made up of genes in the form of DNA strands which contain coded messages that guide the cells about the work that they have to perform. This is how the information about the presence of a dead cell is sent to the brain, and then the cells undergo a process of cell division [25]. This process of cell division gets misled sometimes and hence, the cells start growing rapidly which results in the formation of a lump or blood clot which causes cancer. When it is discovered by the doctors, it is already in the stage where there is no

treatment that can help with the recovery. Therefore, simply cancer is the growth of cells in an abnormal way that changes the gene replication and eventually becomes a multi-cell system that disturbs the cell replication in the body. It then ultimately transforms into a huge group of cells that it can invade any tissue in the body. So, early detection of cancer is very important. Generally, people use detection techniques like PET-CT (positron emission tomography-computed tomography), MRI (Magnetic Resonance Imaging), Biopsy, X-ray, CT scan etc. to detect the presence of cancer in the body but they have limitations like it is slow, complicated, inefficient procedure, with a lots of radiation exposure, and needs of a lot of trained people to operate the equipment making it more expensive.

Recently, many sensing techniques for detection of cancer have been found. Some of them are Colometric biosensors; Fluorescence based biosensor; Plasmon Resonance based sensing; PCF based sensor, grating and interferometer-based biosensor. Among all these sensors, SPR based sensor is considered very efficient due to its label-free sensing technique and delivers a high sensitivity toward its analytes. The SPR based PCF biosensor uses the refractive indices of the healthy and infected cells of different types of cancers which are shown in Table 7.1.

Table 7.1: Refractive Indices of different types of Cancers

Cancer Type	Skin	Blood	Adrenal Gland	Cervical	Breast cancer-Type1	Breast cancer-Type 2
Name of the cell	Basal	Jurkat	PC12	HeLa	MDA-MB231	MCF7
RI of healthy cell	1.360	1.376	1.381	1.368	1.385	1.387
RI of unhealthy cell	1.380	1.390	1.395	1.392	1.399	1.401

7.3. Urinary Tract Infection (UTI)

UTIs are the bacterial infections which affect kidneys, bladder, urethra, and ureters. It can be caused by both gram-positive and gram-negative microorganisms, with *Escherichia coli* (*E. coli*) being the most common gram-negative bacteria, typically found in the gastrointestinal tract. Other bacteria leading to UTIs include *Enterococcus faecalis*

(*E. faecalis*), *Pseudomonas aeruginosa*, *Klebsiella pneumoniae*, and *Staphylococcus saprophyticus* [26]. Approximately 150 million people are affected by UTIs each year, with women being more affected than men. UTI is more frequently encountered during pregnancy, due to the anatomical and physiological variations that take place in the genitourinary tract. The high occurrence of UTIs during pregnancy can lead to various complications, including hypertensive disorders, premature birth, anemia, kidney failure, and low weight infants. The timely identification and treatment of UTIs are crucial in minimizing maternal morbidity and the risk of recurrence. Traditionally, UTIs are diagnosed on conventional techniques like urine microscopy, culturing, and Isothermal microcalorimetry. In clinical trials, urine culture is the most cost-effective method, it is labor-intensive, and time-consuming. To overcome these challenges, fast detection techniques such as ELISA, and PCR are used [27]. They reduce the analysis time, but still demand skilled pathologists and expensive equipment for examination. So, there's a growing demand for reliable, simple, rapid, cost-friendly, and highly sensitive diagnostic tools for UTI, which leads to the development of biosensors. SPR-based sensors offer advantages over conventional sensors for detecting biological interactions. SPR is a quantum optical process enabling direct, sensitive and label-free detection of biomolecular interactions. In an SPR-based sensor, a thin metal film serves a dual role, i.e. interacting with biomolecular ligands on one side and with IR light on the other. Target molecules interacting with the probes produce changes in optical properties, changing the angle of reflection. SPR finds diverse applications, encompassing the assay of antibodies, antigens, bacteria, viruses, DNA, RNA, hemoglobin, hormones, and proteins, with potential future applications. This label-free detection method offers high sensitivity, and enables real-time monitoring of biomolecular interactions. In addition, SPR sensors provide many advantages, such as high accuracy, rapid analysis, and low detection limits, making them highly valuable for a wide range of applications, which includes biosensing, chemical sensing, and environmental monitoring.

UTI is investigated using a different set of urine samples, including both infected and uninfected samples, and identifying the specific pathogen responsible. The response of an established uninfected urine sample with a RI of 1.335 is initially evaluated, and this resonance wavelength is taken as the reference point for infected analyses. The RI of infected samples varies depending upon the type of pathogen causing the infection. For UTI detection, three separate samples infected with different pathogens, have refractive

indices of 1.371 for *Pseudomonas*, 1.388 for *E. coli*, and 1.3921 for *Faecalis*. Taking the established resonance wavelength as a reference point, deviations from this value offer valuable insights into the specific type of pathogen infecting the corresponding samples. Any deviations from the reference point indicate the presence of the particular type of pathogen infection within the sample.

8

Numerical Analysis

8.1. Introduction

The field of optics is advancing at a rapid rate. This growth is proportional to the advantages that an optical provide in terms of bandwidth, higher sensitivity, efficiency and security. It is done by the researchers who are carrying out an extensive research, across the world. Research through experimental setups requires a huge cost, which is economically impractical. So, various optical simulation software have been developed which are based on various numerical techniques. These simulation software helps in making the calculation error free and easier. This simulation software can also define various properties that are essential in defining a PCF, like effective mode index, CL, effective mode area (EMA), effective material loss, birefringence (B), non-linearity, etc.

8.2. Properties Defining a PCF

1. Effective Mode Index

The light propagating through the fiber, travels through an average RI determined by the PCF's design. This average RI is referred as the effective mode index, and can be evaluated using [28]:

$$n_{\text{eff}} = \frac{\beta\lambda}{2\pi} \quad (8.1)$$

2. Confinement Loss (CL)

Due to many factors, light energy escapes from the core, and CL is the measure of this power loss, which is analysed using [29]:

$$\text{CL} \left(\frac{\text{dB}}{\text{cm}} \right) = 8.868 \times \frac{2\pi}{\lambda} \times \text{Im}(n_{\text{eff}}) \times 10^4 \quad (8.2)$$

where, λ is the wavelength and Im is the imaginary part of effective mode index (n_{eff}).

3. Effective Mode Area (EMA)

It is the key sensing zone of a PCF. Spatial distribution of the guided mode is attributed by EMA. It is given by [30], where E is the electric field:

$$EMA = \frac{(\iint |E|^2 dx dy)^2}{\iint |E|^4 dx dy} \quad (8.3)$$

4. Birefringence

In sensing applications, achieving a high birefringence is essential. Maintaining polarization is crucial to decrease the effect of polarization mode dispersion, and to ensure the stable operation of the PCF [31]. It is the absolute value of difference in Ris of two X and Y polarization modes [32]:

$$B = |n_{\text{eff}}^x - n_{\text{eff}}^y| \quad (8.4)$$

5. Sensitivity Measurements

The performance of the sensors can be calculated in two ways, that are, wavelength and amplitude sensitivities. The wavelength sensitivity can be given by [33]:

$$S_w \left(\frac{\text{nm}}{\text{RIU}} \right) = \frac{\Delta \lambda_{\text{peak}}}{\Delta n_a} \quad (8.5)$$

where, $\Delta \lambda_{\text{peak}}$ is the change in wavelengths for different RIs and Δn_a is change in the RIs. The amplitude sensitivity is given by [34]:

$$S_A(\lambda) = -\frac{1}{\alpha(\lambda, n_a)} \frac{\partial \alpha(\lambda, n_a)}{\partial n_a} \quad (8.6)$$

Where $\alpha(\lambda, n_a)$ is loss at a particular wavelength, $\partial \alpha(\lambda, n_a)$ is difference between two loss spectra, and ∂n_a is the change in RIs in the analyte.

8.3. Simulation Software

Optical simulation software are used with optical components like fibers, photonic devices, opto-electronic systems, waveguides etc. With the help of these

simulation software, researchers are able to design components as well as are able to optimize them for better performance. The software are based on numerical methods like FEM, transfer matrix method, finite difference time domain (FDTD) method etc. Every software has inbuilt modules to solve different simulations with high efficiency.

Multiphysics software such as COMSOL Multiphysics, RP Fiber, and Ansys Multiphysics are instrumental in simulating fiber designs and assessing their performance. These simulations allow for a comprehensive analysis of fiber properties and behavior under various conditions.

8.3.1. COMSOL Multiphysics Software

COMSOL Multiphysics is a software which can be used as finite element analysis, solver, and simulation software package for many different physics and engineering applications, especially in coupled phenomena and multi physics. The software uses a conventional physics-based user interfaces and coupled systems of partial differential equations (PDEs). COMSOL provides an IDE and unified workflow for electrical, mechanical, fluid, acoustics, optics and chemical applications. COMSOL can be used for the analysis of the following

- a) Linear and non-linear analysis
- b) Stationary and Time-dependent studies
- c) Frequency domain, modal, Eigen frequency, boundary mode analysis etc.

In the optical domain the software is be used to perform both ray and wave optics analysis with the inbuilt modules and can be used to design as well as simulate antennas, optical fibers, metamaterials, photonic waveguides etc.



Fig 8.1. COMSOL Multiphysics Software

[Image via www.everythingrf.com]

8.4. Numerical Analysis

The simulation software are equipped with the algorithms which are used to numerically analyse the proposed fiber designs and also to evaluate their performance. These software use various mathematical methods to conduct comprehensive analysis of the fiber. Some of these methods are discussed below.

8.4.1. Finite Element Method (FEM)

The FEM is a technique used to numerically obtain the approximate solutions for boundary value problems with PDEs. FEM achieves this by partitioning a complex problem into smaller, more manageable components known as finite elements. The physical structure is divided into a finite number of subdomains, called elements, who are interconnected at points known as nodes. This process is also known as meshing.

8.4.2. Finite Difference Time Domain Method

The FDTD method is a computational technique used to simulate models in one, two, and three dimensions. They were initially created to address hydrodynamics problems, FDTD discretizes differential equations into difference equations using central difference approximations. The key steps involved in FDTD include:

1. Divide the solution region into nodes, with a finer grid yielding more accurate results.
2. Approximating the given differential equation as a difference equation using central difference approximations, which relate the value of the dependent variable at a specific point to its values at neighbouring points.
3. Solving the resulting difference equation iteratively in a leapfrog manner, subject to the prescribed boundary conditions.

Highly Sensitive Black Phosphorus– Layered SPR-PCF Refractometric Sensor ¹

9

9.1. Introduction

SPR is a phenomenon that occurs at the surfaces of the metals (like gold, silver), whenever electrons interact with light beam that strikes the surface at a particular angle. The interaction is sensitive to the changes in the nearby environment, or simply the changes in RI. On comparing with the traditional sensing methods, the sensing technology adopting SPR technique has advantages of real time analysis; it is much more sensitive to the changes in surroundings, and is label free. Therefore, SPR sensing approach has proved as remarkable detection technique due to higher sensitivity and a vast number of applications like biosensing, antibody interaction, clinical trials, food quality analysis, and gas detection.

PCFs are special types of optical fibers which have tiny air holes running along its length. These air holes control how the light moves throughout the fiber. It is possible to manipulate the light propagation more precisely with PCFs than with traditional fibers. PCFs have the advantages of high birefringence, higher nonlinearity, and flexible structural design. These properties give rise to a large number of applications like terahertz communication [7], terahertz-based sensors [8, 34], RI sensors [9], pressure sensors [10], electric and magnetic field sensor [11], supercontinuum generation [35–37], high-power fiber lasers, fiber components for metrology and spectroscopy, etc.

PCF-based SPR sensors arise as types of sensors that are used to detect tiny amounts of substances in various domains such as biology, environment, and medicine. Looking at its advantages, such as smaller size, single mode propagation, effortless light

¹ A part of the results presented in this chapter have been reported in a research publication:

Gupta, P., Khamaru, A., & Kumar, A. (2025). Highly Sensitive Black Phosphorus–Layered SPR-PCF Refractometric Sensor. *Plasmonics*. (Article, in press)
<https://doi.org/10.1007/s11468-024-02723-5>

launching, and ability to control evanescent field penetration, have made it a promising candidate for sensing. The light enters and travels through the core of the PCF and as the light strikes the plasmonic material (like silver, gold), it causes electrons in the metals to oscillate. A strong interaction happens when light and electron oscillations match up and the phenomena is known as resonance. If the environment around the fiber changes, or RI of the analyte changes, the resonance condition shifts. This shift changes the incident light's wavelength, which a PCF-SPR sensor can detect. Even a tiny amount of change in surrounding environment will be noticed by a very sensitive PCF-SPR sensor. They are mainly investigated numerically or analytically using a simulation technique, known as FEM via COMSOL software.

Graphene, silicene, germanene, phosphorene and BP are reported to possess plasmonic properties [18-20]. BP is a new type of 2-D plasmonic material that is attracting the attention of researchers due to its electrical and optical properties which include direct band gap, smaller work function, high charge carrier mobility, and better binding of molecules on the surface of sensors [21].

A TiO₂/Gold/BP layered configuration-based, D-shaped RI sensor is proposed in this work. TiO₂ film works as an adhesive agent between the PCF body and plasmonic material [38]. Gold is the most favorable plasmonic material because of its chemical stability and corrosion resistance against different environments [38]. It also allows a large shift in peak resonance wavelength. BP nano-films are used to elevate the sensor's sensitivity. Numerous smaller air holes are kept near the fiber core, which helps to squeeze the maximum energy of the core mode to couple with the plasmonic metal, and hence enhances the sensitivity of the sensor [40]. Moreover, the structural parameters, like thickness of TiO₂ and gold layer, and number of BP layers are optimized to achieve better sensing performance of the proposed sensor.

9.2. Structural Parameters

The proposed D-shaped SPR-PCF biosensor's cross-section view, and magnified view is shown in Fig 9.1(a). The PCF structure consists of two types of air holes distributed in the cladding in triangular lattice. The bigger air holes having radius, $r_1=1\ \mu\text{m}$ are distributed in the cladding. The smaller air holes with radius, $r_2=0.3\mu\text{m}$ are placed near the fiber core in such a way that the distribution forms an inverted triangular

core. The plasmonic metal layer, that is gold of thickness, $t_{Au}=35$ nm is layered on the flat surface of the D-shape PCF sensor. Along with gold, TiO_2 of thickness, $t_{Ti}=14$ nm, is used plasmonic metal film and also works as wavelength sensitivity enhancer. To elevate the sensitivity to a greater extent, a definite number of layers of BP each of thickness $t_{BP}=0.53$ nm is layered above the plasmonic materials. The RI of the measured medium, that is analyte of thickness $t_a = 1.5\mu m$, is defined as n_a . Fig 9.1(b) represents the schematic diagram for the experimental setup. The light is transmitted to the proposed D-shaped PCF from a broadband source and through a single mode fiber (SMF). The light then passes through the optical spectrum analyzer (OSA) which is connected to the PCF from the other end. Further, the data is collected using a computer.

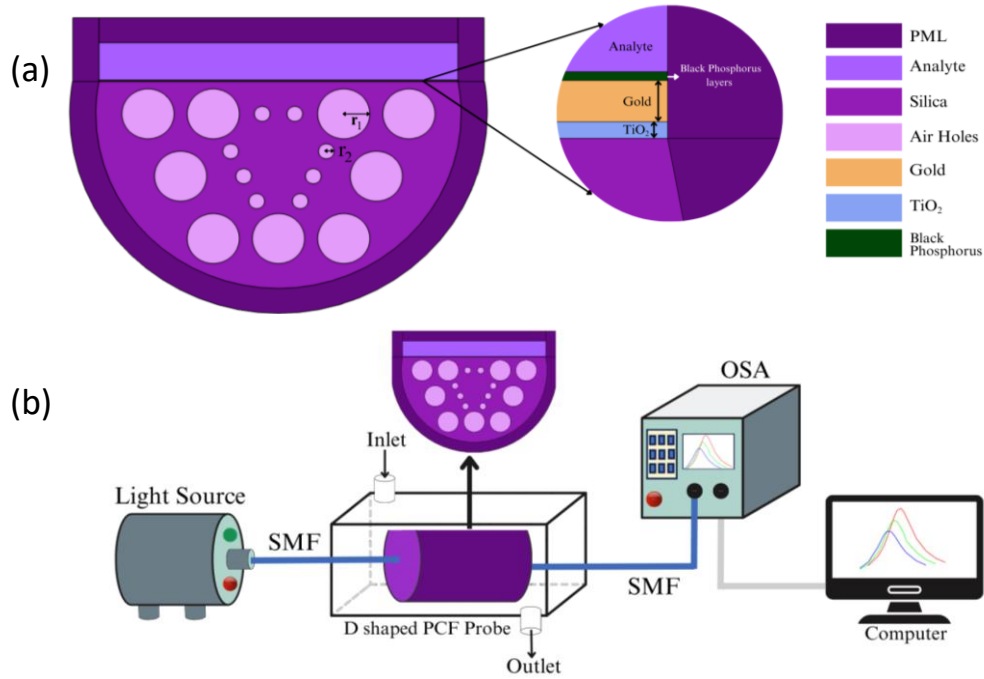


Fig.9.1. (a) Cross section of proposed D-shaped PCF SPR Sensor (b) Schematic diagram for experimental setup

9.3. Methodology

The plasmonic metal consists of two kinds of electrons, that are free electrons and bound electrons. Paul Drude gave the Drude Model for free electrons and Hendrik Lorentz gave the Lorentz Oscillator model for bound electrons, which are used to find the dielectric constant of the metal, i.e. gold. The combined model is known as Drude Lorentz Model, which is then used to find the RI of the metal [38].

$$\epsilon_{Au} = \epsilon_{\infty} - \frac{\omega_D^2}{\omega(\omega + j\gamma_D)} - \frac{\Delta\epsilon \Omega_L^2}{\omega^2 - \Omega_L^2 + j\Gamma_L\omega} \quad (9.1)$$

Here, ϵ_{∞} is the permittivity at high frequency having the magnitude 5.9673 that occurs when electric field of the light, i.e. an electromagnetic wave is very high and the electrons cannot respond to that. γ_D is the damping factor as free electrons cannot keep moving forever and attain the magnitude $\sim 2\pi \times 15.92$ THz, ω_D ($\sim 2\pi \times 2113.6$ THz) is the frequency by which the free electrons in the metal oscillate when disturbed by light. ω is the frequency of light, which, in the case of an RI sensor, depends on the wavelength of the light. Γ_L ($\sim 2\pi \times 104.86$ THz) is the damping factor for bound electrons, Ω_L ($\sim 2\pi \times 650.07$ THz) is the frequency of bound electrons which are vibrating when light hits them, and $\Delta\epsilon$ is the change in permittivity occurred due to the vibrations of bound electrons.

The material used for the composition of the PCF is pure silica, and as its RI is a function of wavelength, therefore wavelength-dependent Sellmeier equation is used,

$$n^2(\lambda) = 1 + \frac{D_1\lambda^2}{\lambda^2 - E_1} + \frac{D_2\lambda^2}{\lambda^2 - E_2} + \frac{D_3\lambda^2}{\lambda^2 - E_3} \quad (9.2)$$

where λ is the wavelength of light and D_i, E_i are constants with $D_1=0.696163$, $D_2=0.4079426$, $D_3=0.8974794$, $E_1=0.0684043$, $E_2=0.1162414$, $E_3=9.896161$.

A thin layer of TiO_2 is incorporated just above the gold layer to act as an adhesive agent between PCF structure and plasmonic film. The RI of TiO_2 is calculated using the given wavelength-dependent formula, where λ is in the Å units [41]:

$$n^2 = 5.913 + \frac{0.2441}{\lambda^2 - 0.0803} \quad (9.3)$$

The RI of BP used in the structure is measured using the Cauchy absorbent Model [42], where λ is in nm units. The layers of BP are introduced to enhance the sensitivity.

$$n(\lambda) = P + Q \frac{10^4}{\lambda^2} + R \frac{10^9}{\lambda^4} \quad (9.4)$$

$$k(\lambda) = X 10^{-5} + Y \frac{10^4}{\lambda^2} + Z \frac{10^9}{\lambda^4} \quad (9.5)$$

Here, $n(\lambda)$ is the real, and $k(\lambda)$ is the imaginary part of the RI, and $P=3.57$, $Q=6.79$, $R=39.99$, $X=3206$, $Y=-0.521$, and $Z=10.26$ are constants.

9.4. Results and Discussions

In this section, the analysis of simulated results is discussed, with all the possible combinations of structural parameters to increase the sensitivity of the sensor.

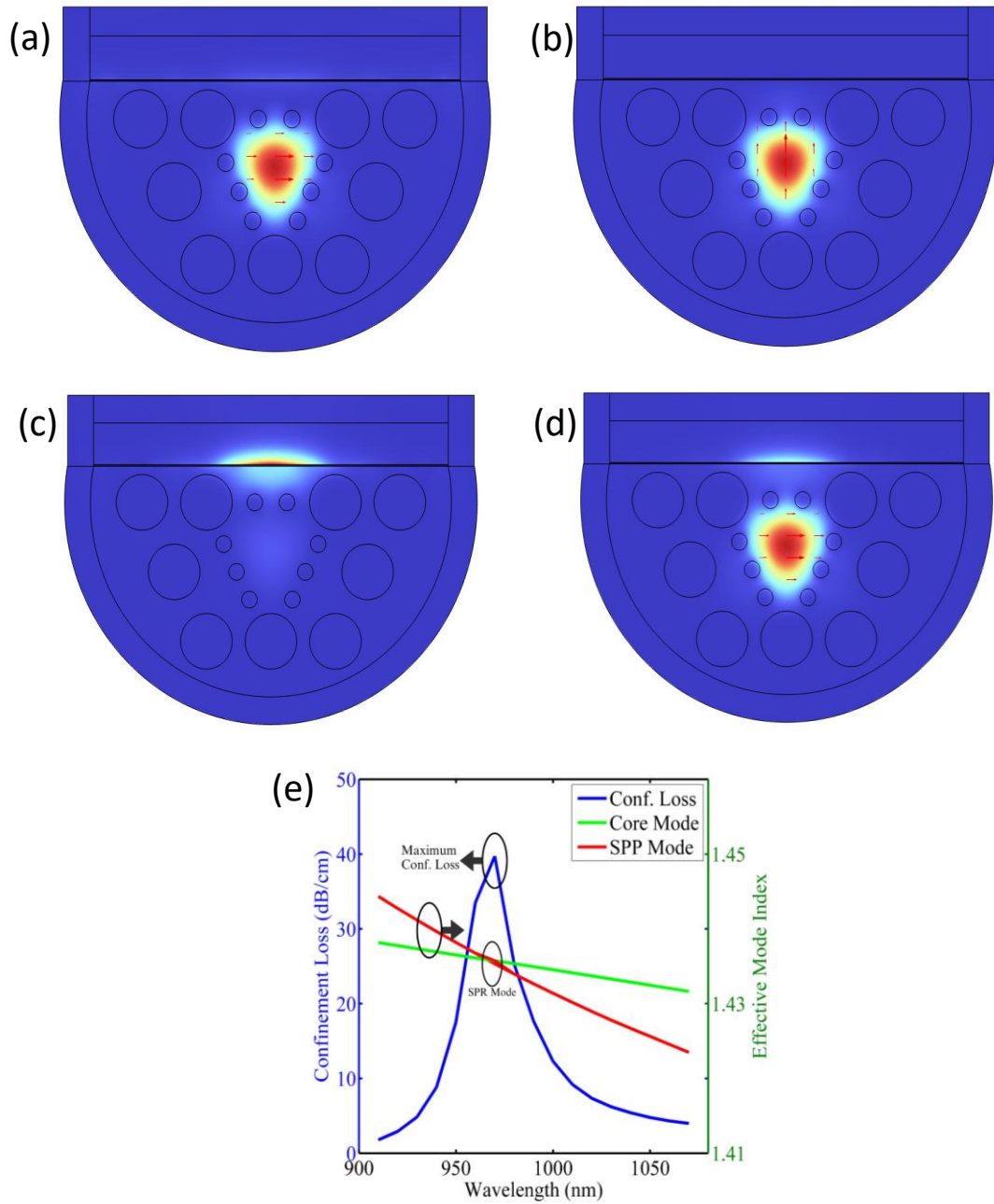


Fig 9.2. Electric field distribution for (a) x-polarized core mode (b) y-polarized core mode (c) SPP mode (d) coupled mode (e) dispersion relation for the optimized structure at 1.38

The electric field distribution of x and y-polarized core mode is shown in Figure 9.2(a) and (b) respectively. The Surface Polariton Mode (SPP), shown in Figure 9.2(c), is the mode where light waves travel along the interface of the metal and the PCF structure. When the coupling between core mode and SPP mode takes place, it enables the respective sensor to detect sensitive changes in the RI or surrounding environment. This is known as coupling mode and also defined as SPR mode (Figure 9.2(d)). Figure 9.2(e) represents the loss curve and dispersion relation for the proposed sensor at RI of 1.38 for analyte. As the resonance takes place between the core mode and SPP mode, the loss increases with increase in wavelength and reaches to maximum value of 39.72 dB/cm at the resonant wavelength of 970nm. At the resonant point, the RI of core mode and SPP mode intersect and maximum light gets coupled with the metal interface.

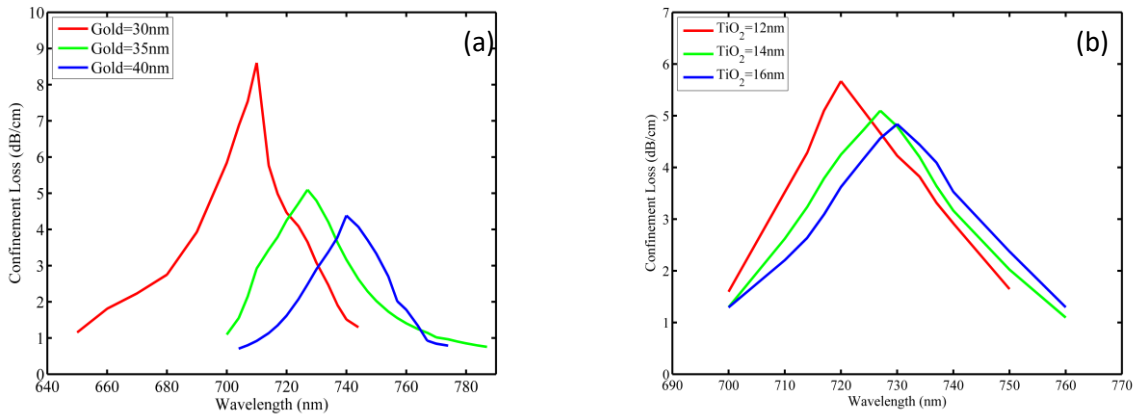


Fig 9.3. Shifts in loss peak at $n_a = 1.38$ (a) with Gold layer thickness (b) with TiO₂ layer

The gold layer thickness is varied from 30 nm to 40 nm at a rate of 5 nm by keeping other parameters constant as $t_{Ti} = 14$ nm, $r_1 = 1$ μ m, $r_1 = 0.3$ μ m. The loss peaks are 8.6, 5.09, and 4.38 dB/cm with the gold layer thickness of 30 nm, 35 nm, and 40 nm respectively as shown in Fig 9.3(a). To consider a favourable spectral width of resonance peak and moderate loss value, 35 nm is chosen as the optimized gold layer thickness. The second optimization step is performed by optimizing the thickness of TiO₂ plasmonic layers. The thickness of TiO₂ is assumed from 12 nm to 16 nm at a changing rate of 2 nm. The allover loss relationship analysis is displayed in Fig 9.3(b).

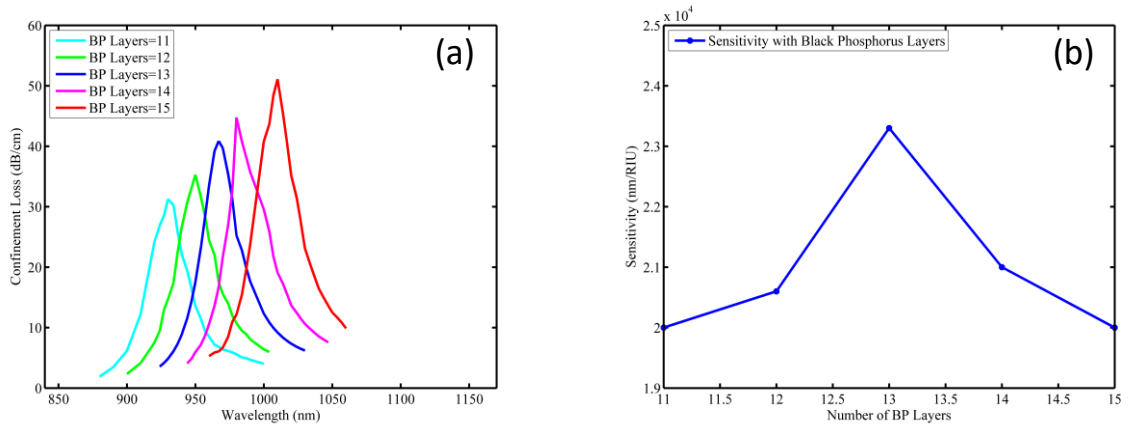


Fig 9.4. (a) Shifts in loss peak at $n_a = 1.38$ with different BP layers and (b) sensitivity variation with BP layers for $n_a = 1.39$

The thickness of single BP layer is defined as 0.53 nm, which distinguishes the material as a 2-D plasmonic material. The loss profiles for embodied 11, 12, 13, 14 and 15 BP layers above the pre-applied plasmonic material (gold+TiO₂) are calculated as 31.25 dB/cm, 35.29 dB/cm, 40.86 dB/cm, 44.77 dB/cm, and 51.09 dB/cm respectively as shown in Fig 9.4(a). With the introduction of 13 layered BP film, the loss profile provides a moderate peak loss. Apart from loss curve, the respective sensitivity of 1.38 RI analyte is also measured at every embraced BP layer combination (11-15 layers at a period of 1). The observation displays that the sensitivity keeps on increasing and increased up to 13 layers of BP but starts decreasing afterwards (beyond 13 layers). The variation in the sensitivity with definite layers of BP is exhibited in Fig 9.4(b). Due to moderate loss peak and enhanced wavelength spectral sensitivity, 13 layers of BP is considered as optimized. The fabrication of BP layers is already covered in the introduction.

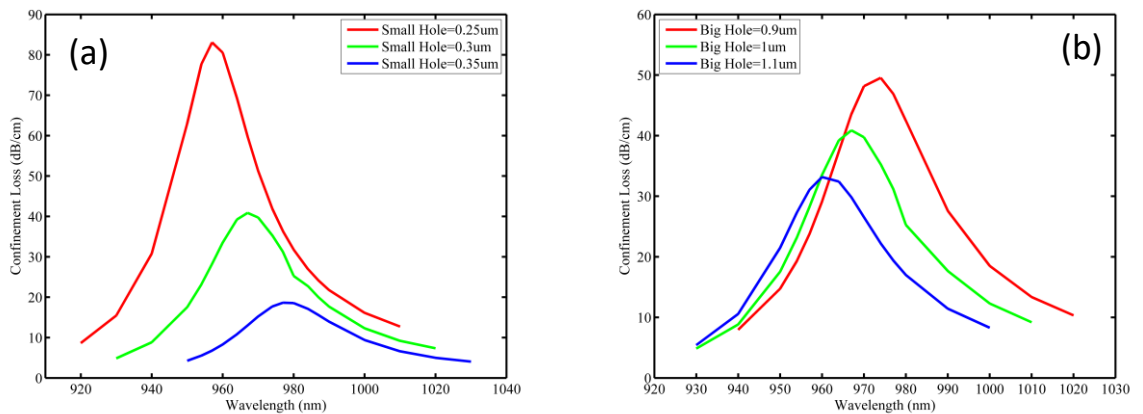


Fig 9.5. Shifts in loss peak at $n_a = 1.38$ (a) with different small air hole radius (b) with different big air hole radius

The effect of smaller air holes results more prominent than bigger air holes because the mode field of core directly interacts with the smaller air holes. To investigate the prominent variation, the smaller air holes radius is changed from $0.25\mu\text{m}$ to $0.35\mu\text{m}$ in the interval of $0.05\mu\text{m}$ and the corresponding confinement peak losses are calculated as 83.06 dB/cm, 40.86 dB/cm, and 18.63 dB/cm respectively, shown in Fig 9.5(a). On changing the diameter of bigger air hole from $0.9\mu\text{m}$ to $1.1\mu\text{m}$ in the step size of $0.1\mu\text{m}$ shows the CL of 49.52 dB/cm, 40.86 dB/cm and 33.16 dB/cm respectively in Fig 9.5(b).

The study provides the spectral CL profiles as shown in Fig.6, for different RI of analyte ranging from 1.3 to 1.4 with a step size of 0.01. BP is proved to increase the sensitivity of the sensor as for the proposed structure, the dynamic sensitivity without depositing BP layers came as 9,000 nm/RIU, and after incorporating BP layers is 23,300 RIU/nm which is higher than the results reported in previous studies [17]. Figure 9.6(a) and 9.6(b) show the loss curves and amplitude sensitivity respectively for the proposed PCF sensor without BP and Figure 9.6(c), and 9.6(d) for the sensor with BP.

The variation of resonant wavelength and analyte's RI are plotting in a graph (Fig 9.7) in which a fourth order polynomial is fitted with coefficients that are tabulated in Table 9.1. The R-square value of fitted curve approximately equals to unity for both the analyses (with BP and without BP).

Table 9.1: Coefficients of fitted polynomial for the curve of Resonant Wavelength vs Analyte's RI

4 th Order Polynomial	$p1 \times x^4 + p2 \times x^3 + p3 \times x^2 + p4 \times x + p5$		
	Without BP	With BP	
p1	3.788e+06	2.325e+07	Polynomial Coefficients
p2	-2.008e+07	-1.243e+08	
p3	3.991e+07	2.491e+08	
p4	-3.527e+07	-2.219e+08	
p5	1.169e+07	7.411e+07	
R ²	0.9985	0.9981	Goodness of fit

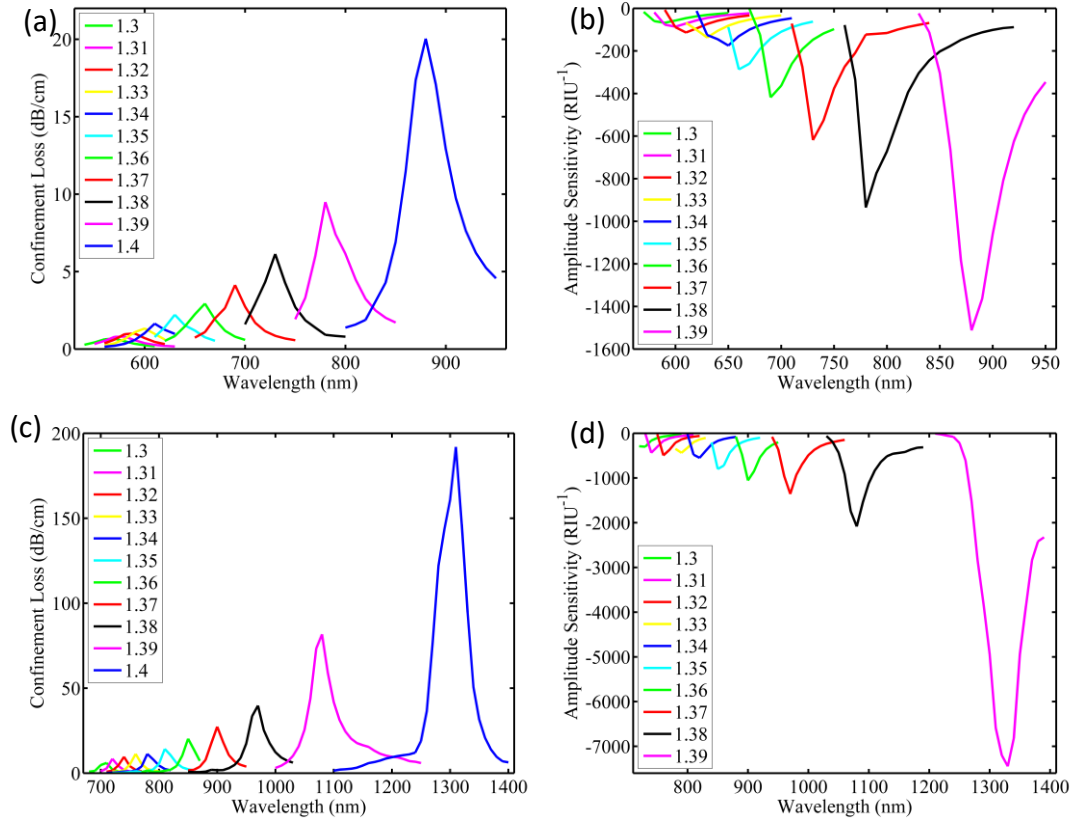


Fig 9.6. (a) Loss Curve and (b) amplitude sensitivity for the optimized parameters without Black Phosphorus. (c) Loss Curve and (d) amplitude sensitivity for optimized parameters with 13 layers of Black Phosphorus.

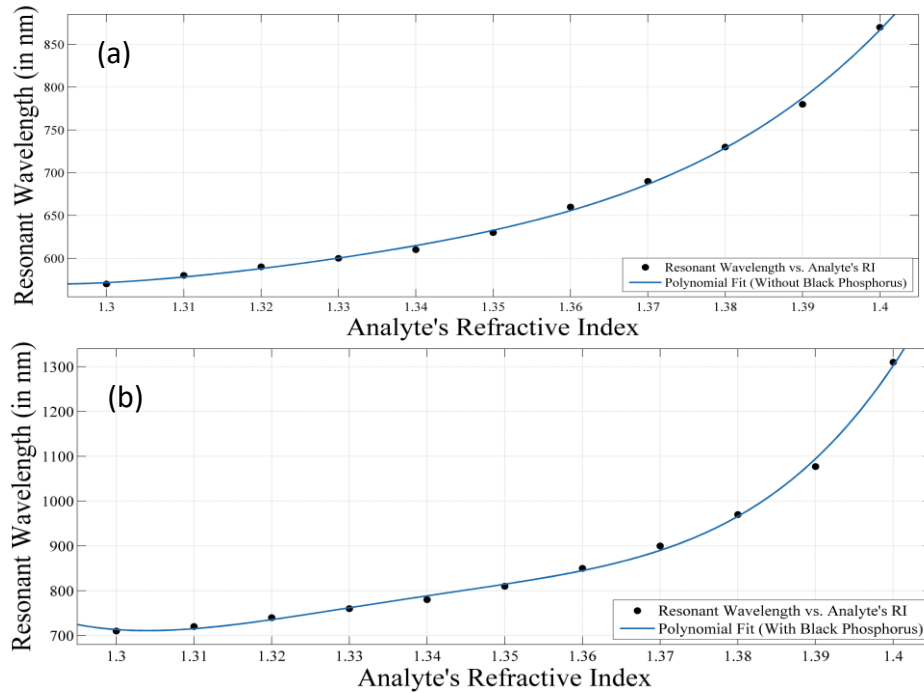


Fig 9.7. Polynomial fitting of resonant wavelength with corresponding RI (a) Without BP (b) With BP

The literature comparison of the proposed sensor with previous works is presented in Table 9.2. The comparison shows a very high increase in dynamic sensitivity for the proposed PCF-SPR Sensor. It also includes the comparison of the sensor with and without plasmonic material i.e. BP and shows that the sensor becomes more than twice sensitive to the changes in the surrounding environment.

Table 9.2. Sensitivity Comparison for the proposed SPR-PCF sensor

Design	Coupling Wavelength (nm)	RI Range	Dynamic Sensitivity (nm/RIU)
Gold and TiO ₂ based SPR-PCF [3]	750	1.35-1.4	10,000
Graphene Based PCF Sensor [43]	590	1.33-1.35	2,520
AZO coated PCF [44]	1820	1.32-1.34	5,000
Ultra polished PCF with BP [22]	778	1.320-1.375	8,200
Proposed D-shaped PCF (without BP)	870	1.30-1.40	9,000
Proposed D-shaped PCF (with BP)	1310	1.30-1.40	23,300

9.5. Conclusion

In summary, the paper presents a D-shaped SPR-PCF refractometric sensor with TiO₂, Gold and BP. BP is a 2-D material which is used to increase the sensitivity of the sensor from 9,000 to 23,300 nm/RIU and amplitude sensitivity of 7446.56 RIU⁻¹ is also achieved. The simulations are performed in COMSOL Multiphysics Software which is based on FEM. All the parameters are optimized to receive such high sensitivity such as

big and small air holes are optimized to be $1\mu\text{m}$ and $0.3\mu\text{m}$ respectively. Similarly, 35nm of Gold Layer, 14nm of TiO_2 and 13 layers of BP are applied to achieve a higher sensitivity. These enhancements make the sensor more appealing to detect even smaller changes in the surrounding environment and are even able to detect a in longer RI sensing range i.e. from 1.3 to 1.4. It can therefore be used in various applications such as medical diagnostics, chemical sensing etc.

Black Phosphorus-Based SPR Photonic Crystal Fiber Biosensor for Urinary Tract Infection Detection ²

10.1. Introduction

UTI is a bacterial infection that affects kidneys, urethra, ureters, and bladders and affects more than 150 million people worldwide annually. The study of UTI varies with age, gender, abnormalities, pregnancy, anatomic, and many other factors. It mostly affects women than men due to anatomical differences in genitourinary tract [26]. According to studies, 3 to 24% of women are affected with UTI during pregnancies which leads to complications such as premature birth, anemia, chronic kidney failure, and lesser birth weight of infants. Generally, conventional methods such as urine culturing, urine microscopy, and other methods like ELISA, PCR, and biosensor detectors are used for UTI detection [27], which are time-consuming, labor intensive, and requires growth media. Therefore, there is a growing demand for simple, rapid, cost-effective, and highly sensitive diagnostic tools to detect UTI, which led to the development of SPR-based biosensors.

Both infected and uninfected samples of urine are used with the objective of detecting as well as identifying the type of pathogen involved in UTI. The data set of uninfected urine sample with a RI of 1.335 is calculated, and that particular resonant point is considered as the reference point for further analysis of different pathogens. The RI of other infected samples depends upon the type of pathogen causing the UTI. The RI is 1.371 for *Pseudomonas*, 1.388 for *E. coli*, and 1.3921 for *E. faecalis*. The deviation

² A part of the results presented in this chapter have been reported in a research publication:

Gupta, Plakshi, Akash Khamaru, and Ajeet Kumar. "Black Phosphorus-Based SPR Photonic Crystal Fiber Biosensor for Urinary Tract Infection Detection." *Plasmonics* (2025). (Article, in press)
<https://doi.org/10.1007/s11468-025-02911-x>

from the reference point indicates the presence of specific pathogen [26,45]. Divya et al. had proposed a dual-channel SPR-based biosensor in 2024 for detection of UTI and TB simultaneously, with a maximum wavelength sensitivity of 8235.29 nm/RIU for UTI [26].

SPR phenomenon and PCFs give rise to SPR-conjugated PCF sensors, which are used to detect even the small substances present in the surroundings of the sensor. It is advantageous as it has smaller size and effortless light launching, and its ability to control the evanescent field penetration has made it an effective technique for sensing. A light beam enters the PCF and penetrates to the core. As the light hits plasmonic material, free electrons present there begin oscillating. A strong interaction happens when the frequency of oscillations and light matches up correctly, called resonance condition. If the RI of the environment or analyte changes, then this resonance condition shifts, which can be easily detected by the SPR-PCF sensor. These changes are detected by the sensor and are investigated numerically or analytically using finite element method in the COMSOL Multiphysics software.

BP possesses a zigzagged-honeycomb structure [21]. BP has great electrical and optical properties which is attracting researchers working on plasmonics. Its properties, like direct band gap, allow it to react with light at specific wavelengths, and a smaller work function allows the electrons to jump easily between the surrounding environment and the BP layer. Higher charge mobility makes the sensor to send signals fast, resulting in rapid detection. Its ability to bind molecules tightly onto the surface of the sensor makes it very useful in biological and chemical sensing [34]. So, BP improves the sensor's ability by providing proteins, DNA, or chemical analytes an active and open site to stick to. BP is incorporated on the surface of the sensor in the form of thin layers of 0.53-nm thickness each [22]. These are some reasons that BP can be used as a plasmonic layer in biological sensors like the proposed UTI sensor.

This work proposes a TiO₂/gold/BP -layered configuration for UTI sensor with square air holes with high wavelength sensitivity. The square air holes provide higher confinement of the core light, focusing the core field only towards the plasmonic layer for effective interaction. Smaller sizes of square air holes are also used near the core, which squeezes the maximum energy of core mode to couple with the metal layers and, therefore, increases the sensitivity of the sensor. Furthermore, structural parameters like

the thickness of TiO_2 , gold, and the number of BP layers are also optimized to achieve a higher sensitivity for the proposed UTI sensor.

10.2. Structural Design

The designed D-shaped SPR-based PCF biosensor with square air holes is displayed in Fig 10.1a with a cross-sectional and magnified view. The PCF geometry is the composition of two sizes of square air holes, situated in the cladding. The bigger square holes have side length of $1.3 \mu\text{m}$ (a), and smaller ones have side length (b) of $0.8 \mu\text{m}$, which are placed near the fiber core such that most of the light from the core is directed towards the metal layers. On the top of the flat surface of the D-shaped fiber, there is a thin layer of TiO_2 of thickness, $t_{\text{Ti}}=16 \text{ nm}$, which sticks the gold layer on the top of it to the fiber. The thickness of the gold layer, placed above the TiO_2 layer, is $t_{\text{g}}=40 \text{ nm}$. It helps in the proper detection of the UTI cells from the urine sample that is made to pass through the analyte. A significant number of BP layers of thickness, $t_{\text{BP}}=0.53 \text{ nm}$ each, placed above the gold layer, to enhance the sensing capability of the sensor. The BP layers stay connected due to the van der Waals forces of attractions present between them. The RI of the medium to be measured here is defined as bio-analyte (n_a), with analyte channel thickness, $t_a=2 \mu\text{m}$, and is placed above the BP layers. To define the computational domain and get rid of the back-reflection effect, a perfectly matched layer (PML) is applied along the cylindrical geometry having width magnitude of $1 \mu\text{m}$.

Fig 10.1b shows a schematic diagram of the proposed experimental setup. The coupling efficiency is first enhanced by putting a light source with a wide IR spectrum into the biosensor using a single-mode fiber (SMF). At the air-core interface, the light is incident in the biosensor and is guided into the core, through the phenomenon of modified TIR (M-TIR). SPR occurs at the boundary of metal surface and the analyte. Whenever a specific molecule that is to be detected is found, the surface of the metal undergoes RI modification, which also causes alteration in the effective RI and result in wavelength shift. These changes are detected by using an OSA, and connecting it to a computer system enables us to collect the data efficiently.

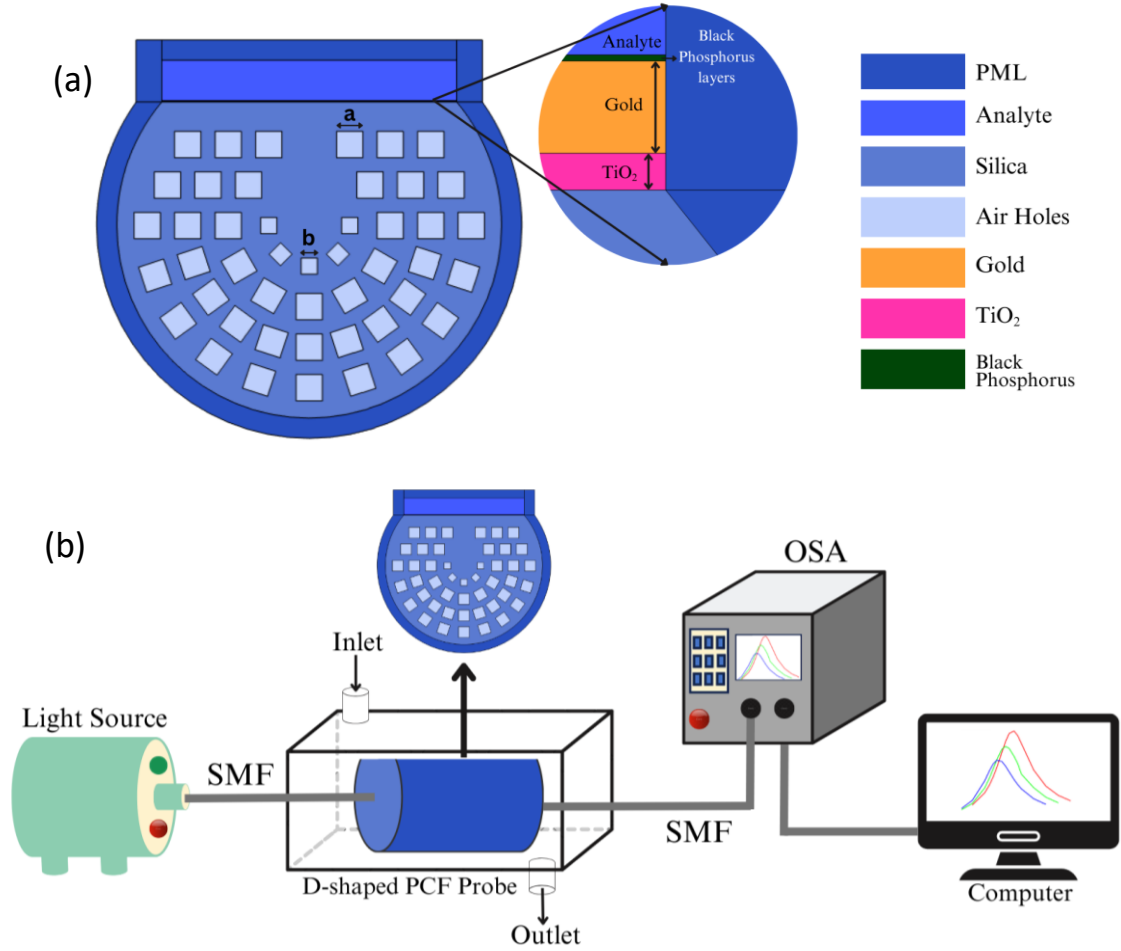


Fig 10.1. (a) Cross-sectional view of proposed D-shaped SPR PCF Biosensor
(b) Experimental setup

10.3. Methodology

The proposed structure is analyzed using the FEM in the COMSOL Multiphysics Software. The PCF is composed of the pure silica material and its RI is a function of wavelength, so Sellmeier equation is used, which is wavelength dependent,

$$n^2(\lambda) = 1 + \frac{D_1\lambda^2}{\lambda^2 - E_1} + \frac{D_2\lambda^2}{\lambda^2 - E_2} + \frac{D_3\lambda^2}{\lambda^2 - E_3} \quad (10.1)$$

here, λ is wavelength of light, and $D_1=0.696163$, $D_2=0.4079426$, $D_3=0.8974794$, $E_1=0.0684043$, $E_2=0.1162414$, $E_3=9.896161$ are constants.

The TiO₂ layer is placed above the gold layer and it acts as an adhesive agent between Gold and the PCF. The RI of the PCF is calculated using the following formula where λ is in Å units [38]:

$$n^2 = 5.913 + \frac{0.2441}{\lambda^2 - 0.0803} \quad (10.2)$$

The Gold metal consists of two types of electrons, free electrons and bound electrons. Drude Model is used find dielectric constant of free electrons and Lorentz Oscillator Model is used for bound electrons. The combined model for dielectric constant of gold metal is known as Drude Lorentz Model [39]:

$$\epsilon_{Au} = \epsilon_{\infty} - \frac{\omega_D^2}{\omega(\omega + j\gamma_D)} - \frac{\Delta\epsilon \Omega_L^2}{\omega^2 - \Omega_L^2 + j\Gamma_L\omega} \quad (10.3)$$

where, $\epsilon_{\infty}=5.9673$ is the permittivity at high frequencies, occurring when electric field of light is high and an electron is not able to respond to it. $\gamma_D \sim 2\pi \times 15.92$ THz is the damping factor as the free electrons cannot move forever. $\omega_D \sim 2\pi \times 2113.6$ THz is the frequency of oscillation of the free electrons in the metal, when light strikes them. ω is the frequency of light. Similarly, $\Gamma_L \sim 2\pi \times 104.86$ THz is the damping factor for bound electrons, $\Omega_L \sim 2\pi \times 650.07$ THz is the frequency of oscillation of bound electrons, when light hits them, and $\Delta\epsilon$ is change in permittivity due to vibration of bound electrons.

The Cauchy Absorbent Model is used to find the RI of the BP layers, where λ is in nm units [42],

$$n(\lambda) = P + Q \frac{10^4}{\lambda^2} + R \frac{10^9}{\lambda^4} \quad (10.4)$$

$$k(\lambda) = X 10^{-5} + Y \frac{10^4}{\lambda^2} + Z \frac{10^9}{\lambda^4} \quad (10.5)$$

where, $n(\lambda)$ is the real and $k(\lambda)$ is the imaginary part of the RI. $P=3.57$, $Q=6.79$, $R=39.99$, $X=3206$, $Y=-0.521$, and $Z=10.26$ are constants.

10.4. Fabrication Feasibility of Proposed Design

The gold layer can be fabricated on the flat surface of the proposed D-shaped sensor by various methods like Pulse Laser Deposition, RF Sputtering, and Splash Technology. In Pulsed Laser Deposition, a pulsed beam of high energy is targeted on the bulk gold, which causes ejection of the gold atoms from the bulk surface [39]. In RF Sputtering technique, radio frequency energy is used to create plasma, that is targeted on the bulk

gold, causing the gold atoms to sputter out. Splash Coating technology involves spraying or splashing liquid gold nanoparticles on the PCF's flat surface, which is then followed by a heat treatment.

The fabrication of TiO_2 can also be done using various methods such as, Chemical Vapour Deposition, Sol-Gel method, Atomic Layer Deposition, etc. [42] But Sol-Gel is the most commonly used method. In this a solution of titanium alkoxide is hydrolyzed and condensed to form a gel of TiO_2 , which is then deposited on the PCF's surface and heat treated subsequently to convert it into a crystalline film.

BP layers can also be prepared by using many different methods such as, mechanical peeling (most commonly used), Liquid Peeling and Pulsed Laser Precipitation [22]. Mechanical Peeling involves the peeling of thin layers of BP from the bulk crystal, physically. It involves a special type of instrument, which can be adjusted according to the thickness of BP required. In Liquid Peeling, a bulk piece of BP is placed in a liquid like water and then ultrasound waves are passed through it. These vibrations cause the layers to come apart and disperse into the liquid. This method is used for preparation of bulk layers. Pulsed Laser precipitation method requires a powerful laser to be fired at the bulk BP and the energy from the laser breaks apart thin layers.

The square air holes can be prepared using the stack and draw method, in which the bundles of silica capillaries are traced down along the length of PCF and mingled. This technique provides mechanical stability as surface tension balances out the drawing process forces. Other than this, the square holes can also be prepared by 3-D printing method and extrusion technique. This technique allows to extract fiber by drawing from bulk glass, and any pattern like circles, squares or rectangles can be formed. Therefore, it can be believed that the fabrication of the proposed biosensor is possible using the mentioned fabrication techniques [46].

10.5. Results and Discussions

The analysis of the proposed sensor using the COMSOL Multiphysics software are discussed and all the combinations of structural parameters to increase the sensitivity are shown.

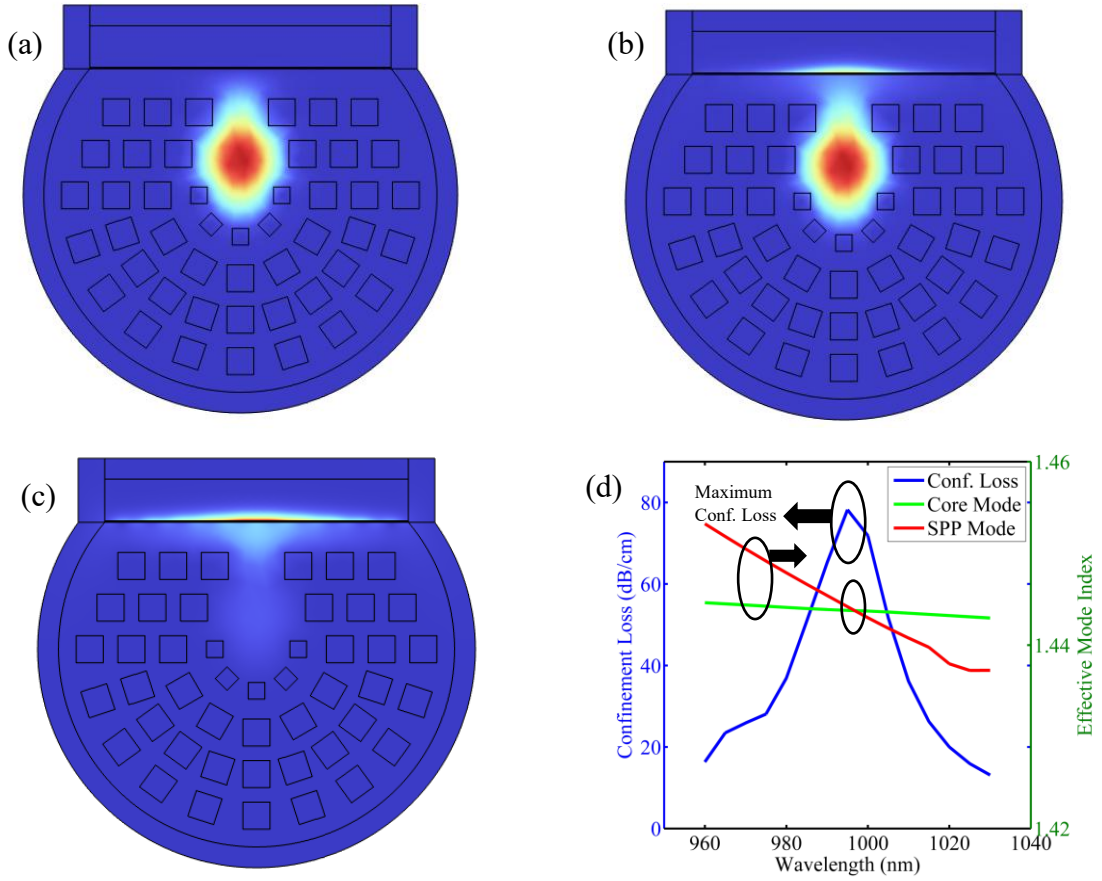


Fig 10.2 (a) Core Mode (b) SPR Mode (c) SPP Mode (d) Effective mode coupling and maximum loss

Fig 10.2(a-c) show Core Mode, coupled mode (SPR Mode) and SPP Mode respectively. Fig 10.2(d) shows the loss curve and dispersion relation for the biosensor at RI 1.335 in the analyte. As the resonance condition comes, the loss increases with increase in wavelength and reaches to a maximum value of 78.22 dB/cm at the wavelength of 995nm. At the resonant point, the RI of the core and SPP mode intersect and maximum light gets coupled with plasmonic materials.

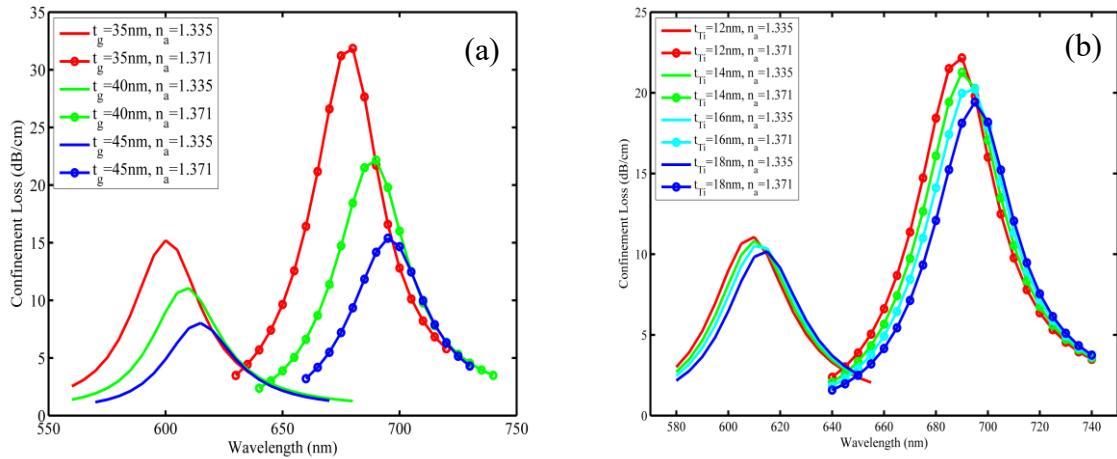


Fig 10.3. Loss Curves for different values of RI with variation of
(a) Gold Layer thickness, (b) TiO₂ Layer Thickness

The optimized thickness of gold layer is investigated by varying t_g from 35nm to 45nm in steps of 5, by keeping other parameters constant. The analysis with BP layers is done separately, so no BP is incorporated this time. Fig 10.3(a) shows the CL spectra of the structure as t_g gradually increases. The results show that the resonant wavelength shifts towards larger wavelengths and the loss of light from core to plasmonic layers decreases, as the t_g increases. The CL spectrum by changing the thickness of TiO₂, from 12nm to 18nm in steps of 2, is shown in Fig 10.3(b). It is analyzed by using the optimized value of gold, i.e. 40nm and keeping other parameters constant. The corresponding sensitivity remains same from 12nm to 14 nm thickness but increases at 16nm and then again decreases at 18nm. So, the ideal thickness of TiO₂ is 16nm.

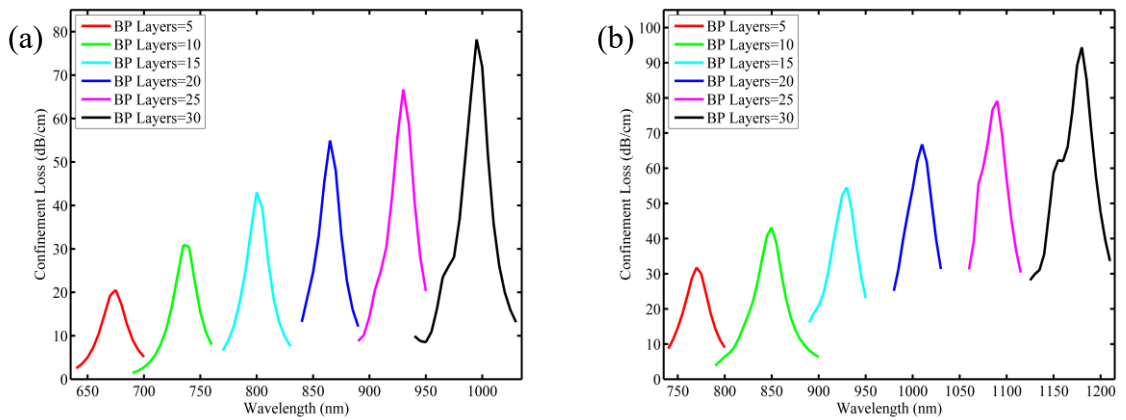


Fig 10.4. Loss Curves for different layers of BP when effective RI is
(a) 1.335 (b) 1.371

To find the ideal number of BP layers, the analysis is done, starting from 5 layers to 30 layers. The sensitivity keeps increasing, and 30 layers are considered to be optimal because beyond this layer, the core modes and SPP modes are not clearly visible. This is because the wavelength range crosses 2500nm (Silica's absorption limit) for higher RI of UTI, that is 1.3921. The CL spectrum for the analysis from 5 to 30 layers of BP is shown in Fig 10.4.

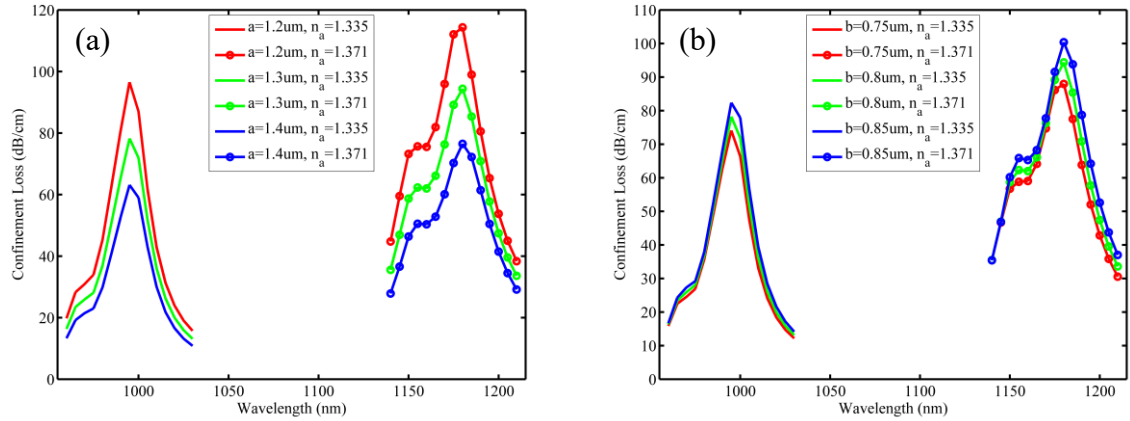


Fig 10.5. Loss Curves for different values of RI with variation of (a) Size of Bigger air hole, (b) Size of Smaller air hole

The CL spectrum is shown in Fig 10.5 (a) and (b) and it can be concluded that the size of air holes is not affecting the sensitivity of the proposed sensor, but the CL gets affected. It decreases for bigger air holes and increases for smaller ones. So, the size with moderate loss, i.e. $a=1.3\mu\text{m}$, and $b=0.8\mu\text{m}$, is considered to be ideal.

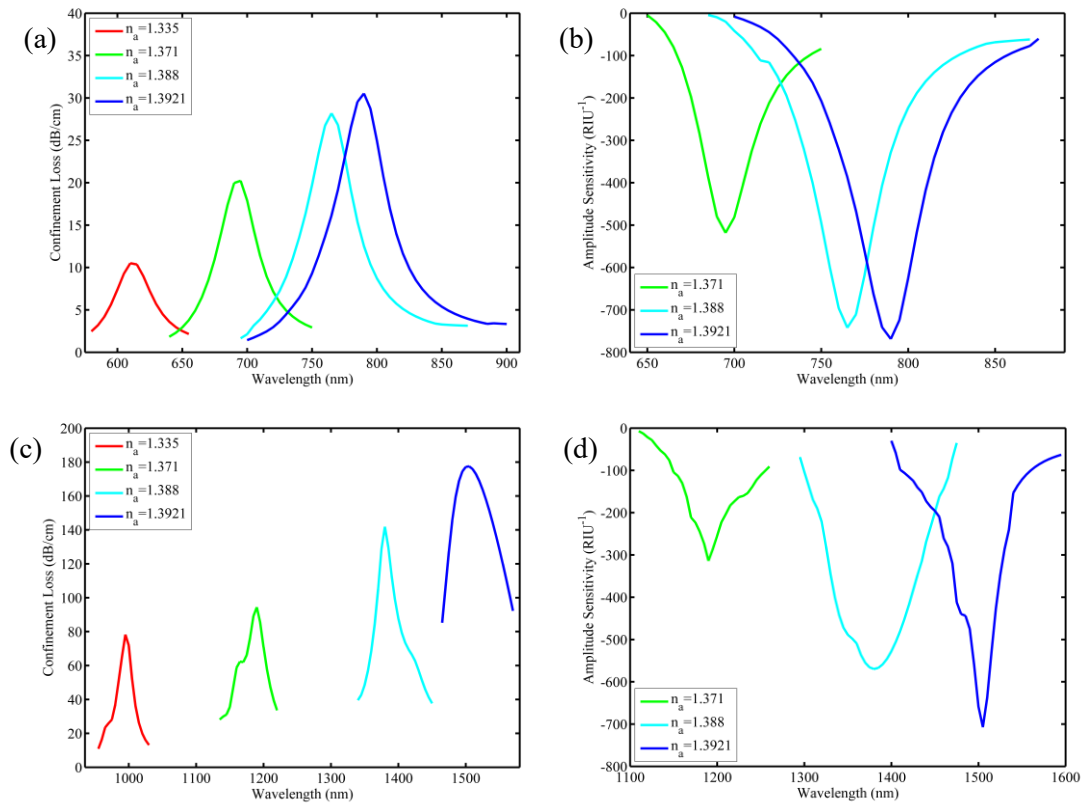


Fig 10.6. Performance of proposed Sensor: CL (a)Without BP (c)With BP
& Amplitude Sensitivity (b)Without BP (d)With BP

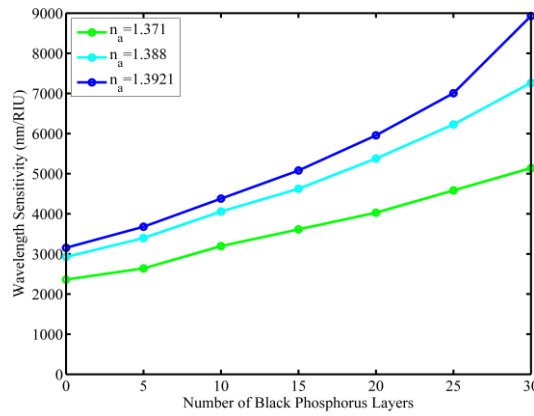


Fig 10.7. Variation in sensitivity with increase in number of BP layers

To look at the final performance of the proposed SPR-PCF UTI sensor, the graphs have been plotted using the RI of the various bacteria of UTI. The performance of the sensor can be measured in two ways, that are by calculating wavelength and amplitude sensitivity. The main objective of this work is to make a highly sensitive UTI sensor which is achieved using the BP layers. So, the analysis is shown without and with BP layers to get a clear observation about the increase in sensitivity. Fig 10.6(a) and (b)

show wavelength and amplitude sensitivity respectively of the proposed structure without BP and Fig 10.6(c) and (d) show the same for the structure with BP. And, Fig 10.7 shows the increase in wavelength sensitivity from 0 layers to 30 layers with an interval of 5.

The performance of the sensor is tabulated in Table 10.1, to show the clear the difference between the sensitivities for the sensor with and without BP layers.

Table 10.1: Change in Wavelength and Amplitude sensitivity when BP layer is added

Analyte's RI	Proposed structure without BP			Proposed structure with BP		
	Resonant Wavelength (nm)	Wavelength Sensitivity (nm/RIU)	Amplitude Sensitivity (RIU ⁻¹)	Resonant Wavelength (nm)	Wavelength Sensitivity (nm/RIU)	Amplitude Sensitivity (RIU ⁻¹)
1.335	610	-	-	995	-	-
1.371	695	2361.11	518.28	1190	5138.88	313.91
1.388	765	2924.52	742.15	1380	7264.15	569.63
1.3921	795	3239.92	768.67	1505	8936.69	707.31

Table 10.2 shows the comparison of the proposed SPR based PCF biosensor with previous literature works.

Table 10.2. Sensitivity Comparison for the proposed SPR-PCF sensor

Design		Coupling Wavelength (nm)	RI Range	Sensitivity (nm/RIU)
Graphene Based Sensor [43]		590	1.33-1.35	2,520
AZO coated Sensor [44]		1820	1.32-1.34	5,000
Dual Channel UTI sensor [26]	Pseudomonas Bacteria	1640	1.371	3888.33
	E. Coli Bacteria	1780	1.388	5283.01

	E. Faecalis Bacteria	1800	1.3921	5253.94
Proposed UTI Sensor (without BP)	Pseudomonas Bacteria	695	1.371	2361.11
	E. Coli Bacteria	765	1.388	2924.52
	E. Faecalis Bacteria	795	1.3921	3239.92
Proposed UTI Sensor (with BP)	Pseudomonas Bacteria	1190	1.371	5138.88
	E. Coli Bacteria	1380	1.388	7264.15
	E. Faecalis Bacteria	1505	1.3921	8936.69

10.6. Conclusion

This research presents a UTI sensor, based of SPR. The UTI has 3 types of bacteria which affects the human body, which are Pseudomonas, E. Coli, and E. Faecalis. The structure is composed of TiO₂ and Gold layers along with BP Layers to increase the sensitivity of the sensor. The structure consists of square air holes of two sizes for better birefringence and non-linearity. All these structural parameters are optimized and the fabrication techniques of the sensor are also present in the paper. The analysis is done by taking the uninfected cell as the reference and the refractive indices of the uninfected and infected cells are also present in the paper. Using this information, a highly sensitive UTI sensor is designed. The analysis is also done by comparing the structure with and without BP. When the sensor is operated without the BP layers the wavelength sensitivity for different types of bacteria are 2361.11, 2924.52, and 3239.92 nm/RIU whereas, when the BP layers are incorporated the sensitivities goes as high as 5138.88, 7264.15, and 8936.69 nm/RIU. This shows that there is an increase in the sensitivities by much more that 50% and hence, a successful UTI Biosensor is designed.

11

Conclusion and Future Scope

11.1. Conclusion

In this work, SPR based PCF sensors have been designed for ultrafast sensing applications. The proposed sensors are RI sensor, and biosensors which are sensitive to the changes in RI of the analyte. The proposed sensors can be used to detect various cancer cells, UTI cells of different bacteria. All the proposed designs are simulated and numerically analysed in the COMSOL Multiphysics Software. Various optical parameters like CL, wavelength sensitivity and amplitude sensitivity are evaluated for analysing the sensor's performance. The proposed RI sensor can sense in the range from 1.3 to 1.4 RI, and therefore can be used in various applications such as medical and chemical sensing. It shows the wavelength sensitivity of 23,300 nm/RIU and an amplitude sensitivity of 7446.56 RIU⁻¹, which shows that the sensor can detect even the small changes in the surrounding environment. The proposed UTI sensor shows the wavelength sensitivities for different bacteria as 5138.88 for *Pseudomonas*, 7264.15 for *E. coli*, and 8936.69 nm/RIU for *E. faecalis*. Similarly, the proposed cancer biosensor shows the wavelength sensitivities as 7142.86 nm/RIU for blood cancer cell, 5000 nm/RIU for skin cancer cell and 8333.33 nm/RIU for cervical cancer cell.

11.2. Scope of Future Work

The present study has laid a foundational framework for advanced photonic device design and biosensing applications using engineered nanostructures and novel materials. Building upon this work, several promising directions can be pursued in the future:

1. **Exploration of Metamaterials for Enhanced Photonic Devices:** Metamaterials, artificially structured materials with unique electromagnetic responses—can be integrated into existing sensor architectures to significantly enhance light-matter interaction. Future work could focus on designing and

simulating metamaterial-based PCFs or integrated platforms to improve sensitivity, miniaturization, and tunability, especially in biosensing and environmental monitoring applications.

2. Incorporating and Characterizing Novel 2D Materials:

While this study has primarily explored materials like BP, there exists substantial scope to expand into other 2D materials such as MXenes, transition metal dichalcogenides (e.g., MoS₂, WS₂), and heterostructures of these materials. These materials offer tunable optical properties, high surface area, and biocompatibility, making them excellent candidates for next-generation photonic and optoelectronic devices.

3. Towards Real-World Applications in Biomedical Diagnostics:

Building upon prior work related to disease detection (e.g., UTI diagnosis or biomarker sensing), future research can explore photonic sensors for a broader range of diseases, such as cancer, neurological disorders, and viral infections. Integration with microfluidics and machine learning can be explored for developing lab-on-chip diagnostic platforms.

REFERENCES

- [1] Rifat, Ahmmed A., et al. "Photonic crystal fiber based plasmonic sensors." *Sensors and Actuators B: Chemical* 243 (2017): 311-325.
- [2] Skorobogatiy, Maksim, and Andrei V. Kabashin. "Photon crystal waveguide-based surface plasmon resonance biosensor." *Applied physics letters* 89.14 (2006).
- [3] Jain, Satyendra, Kuldeep Choudhary, and Santosh Kumar. "Photonic crystal fiber-based SPR sensor for broad range of refractive index sensing applications." *Optical Fiber Technology* 73 (2022): 103030.
- [4] Kumar, Sudhir, and Dilip Kumar. "Sensitivity measurement based on the refractive index detection of dual-coated PCF SPR sensor." *Mapan* 37.2 (2022): 435-441.
- [5] Hoque, Abdullah Mohammad Tanvirul, et al. "U-grooved selectively coated and highly sensitive PCF-SPR sensor for broad range analyte RI detection." *IEEE Access* 11 (2023): 74486-74499.
- [6] Dash, Jitendra Narayan, and Rajan Jha. "Highly sensitive D shaped PCF sensor based on SPR for near IR." *Optical and Quantum Electronics* 48 (2016): 1-7.
- [7] Singh, Gurmeet, Shubham Sharma, and Ajeet Kumar. "Design and analysis of spider-web photonic crystal fiber in the terahertz regime." *Indian Journal of Physics* 98.8 (2024): 2917-2922.
- [8] Singh, Jaydeep, Akash Khamaru, and Ajeet Kumar. "A refractive index based cancer cells sensor in terahertz spectrum: design and analysis." *Journal of Optics* (2024): 1-9.
- [9] Meng, Fanlong, Hong Wang, and Di Fang. "Research on D-shape open-loop PCF temperature refractive index sensor based on SPR effect." *IEEE Photonics Journal* 14.3 (2022): 1-5.
- [10] Lu, Yipeng, et al. "Characteristics of a capillary single core fiber based on SPR for hydraulic pressure sensing." *Optics Communications* 530 (2023): 129125.
- [11] Cennamo, Nunzio, et al. "A magnetic field sensor based on SPR-POF platforms and ferrofluids." *IEEE Transactions on Instrumentation and Measurement* 70 (2020): 1-10.

-
- [12] Yolalmaz, Alim. *Utilization of fiber loop ring down technique for sensing applications*. MS thesis. Middle East Technical University (Turkey), 2017.
- [13] Ritchie, Rufus H. "Plasma losses by fast electrons in thin films." *Physical review* 106.5 (1957): 874.
- [14] Raghuwanshi, Sanjeev Kumar, Santosh Kumar, and Ritesh Kumar. "Application of Geometric-Based SPR Sensors." *Geometric Feature-Based Fiber Optic Surface Plasmon Resonance Sensors*. Singapore: Springer Nature Singapore, 2023. 245-284.
- [15] Bing, Pibin, et al. "Analysis of dual-channel simultaneous detection of photonic crystal fiber sensors." *Plasmonics* 15 (2020): 1071-1076.
- [16] Jabin, Md Asaduzzaman, et al. "Titanium-coated dual-core D-shaped SPR-based PCF for hemoglobin sensing." *Plasmonics* 14.6 (2019): 1601-1610.
- [17] Manickam, Parthiban, and Revathi Senthil. "Numerical investigation of side-polished SPR PCF sensor for urine analysis." *Plasmonics* 17.5 (2022): 2023-2030.
- [18] Vacacela Gomez, C., et al. "Plasmon properties and hybridization effects in silicene." *Physical Review B* 95.8 (2017): 085419.
- [19] Dávila, M. E., et al. "Germanene: a novel two-dimensional germanium allotrope akin to graphene and silicene." *New Journal of Physics* 16.9 (2014): 095002.
- [20] Yuan, Yufeng, et al. "Highly anisotropic black phosphorous-graphene hybrid architecture for ultrasensitive plasmonic biosensing: Theoretical insight." *2D Materials* 5.2 (2018): 025015.
- [21] Qiao, Jingsi, et al. "High-mobility transport anisotropy and linear dichroism in few-layer black phosphorus." *Nature communications* 5.1 (2014): 4475.
- [22] Tong, Kai, et al. "Study on increasing measurement range and enhancing sensitivity of PCF surface-plasmon-resonance biosensor using black phosphorus." *Journal of Russian Laser Research* 42 (2021): 283-291.
- [23] Xing, Chao, et al. "Preparations, properties and applications of low-dimensional black phosphorus." *Chemical Engineering Journal* 370 (2019): 120-135.

- [24] Zhumagaliyeva, G. B., and V. F. Pershin. "Production of few-layer graphene in synthetic oil using a rod drum mill." *Advanced Materials & Technologies* 2 (14) (2019): 59-68.
- [25] Ibrahimi, Khalid Mohd, R. Kumar, and Writtick Pakhira. "Enhance the design and performance analysis of a highly sensitive twin-core PCF SPR biosensor with gold plating for the early detection of cancer cells." *Plasmonics* 18.3 (2023): 995-1006.
- [26] Divya, J., et al. "A novel dual-channel SPR-based PCF biosensor for simultaneous tuberculosis and urinary tract infection diagnosis towards SDG3." *IEEE Access* (2024).
- [27] Gür, Sinem Diken, Monireh Bakhshpour, and Adil Denizli. "Selective detection of Escherichia coli caused UTIs with surface imprinted plasmonic nanoscale sensor." *Materials Science and Engineering: C* 104 (2019): 109869.
- [28] Panda, Abinash, and Puspa Devi Pukhrambam. "Design and analysis of porous core photonic crystal fiber based ethylene glycol sensor operated at infrared wavelengths." *Journal of computational electronics* 20 (2021): 943-957.
- [29] Arif, Md Faizul Huq, et al. "Design and optimization of photonic crystal fiber for liquid sensing applications." *Photonic Sensors* 6 (2016): 279-288.
- [30] Xu, Huizhen, et al. "High numerical aperture photonic crystal fiber with silicon nanocrystals core for optical coherence tomography." *Optik* 219 (2020): 165000.
- [31] Islam, Mohammad Rakibul, et al. "Design of a Topas-based ultrahigh-sensitive PCF biosensor for blood component detection." *Applied Physics A* 127 (2021): 1-16.
- [32] Yadav, Sapana, Pooja Lohia, and D. K. Dwivedi. "A novel approach for identification of cancer cells using a photonic crystal fiber-based sensor in the terahertz regime." *Plasmonics* 18.5 (2023): 1753-1769.
- [33] Liu, Chao, et al. "Symmetrical dual D-shape photonic crystal fibers for surface plasmon resonance sensing." *Optics express* 26.7 (2018): 9039-9049.
- [34] Singh, Neeraj, Akash Khamaru, and Ajeet Kumar. "Design and analysis of a rectangular core refractive index-based PCF sensor for bio-sensing application." *Optical and Quantum Electronics* 56.7 (2024): 1133.

- [35] Tomer, Drishti Singh, and Ajeet Kumar. "A graded index hybrid photonic crystal fiber for supercontinuum generation using AsSe₂-As₂S₅." *Journal of Optics* (2024): 1-10.
- [36] Khamaru, Akash, and Ajeet Kumar. "As₃₈ Se₆₂ based segmented clad-graded index photonic crystal fiber for supercontinuum generation covering 3–9.5 μm with moderate peak power." *Optical and Quantum Electronics* 56.7 (2024): 1246.
- [37] Garg, Deepak, Akash Khamaru, and Ajeet Kumar. "Ge–As–Se–Te chalcogenide based rib-waveguide for highly coherent on-chip mid-infrared supercontinuum generation: design and analysis." *Optical and Quantum Electronics* 56.10 (2024): 1643.
- [38] Ramani, Umang, et al. "Dual-core photonic crystal fiber–based plasmonic sensor for a broad range of refractive index sensing." *Plasmonics* 20.3 (2025): 1551-1561.
- [39] Zuhayer, Asif, et al. "A gold-plated twin core d-formed photonic crystal fiber (PCF) for ultrahigh sensitive applications based on surface plasmon resonance (SPR) approach." *Plasmonics* 17.5 (2022): 2089-2101.
- [40] Singh, Shivam, and Y. K. Prajapati. "Dual-polarized ultrahigh sensitive gold/MoS₂/graphene based D-shaped PCF refractive index sensor in visible to near-IR region." *Optical and Quantum Electronics* 52.1 (2020): 17.
- [41] Singh, Yadvendra, and Sanjeev Kumar Raghuwanshi. "Titanium dioxide (TiO₂) coated optical fiber-based SPR sensor in near-infrared region with bimetallic structure for enhanced sensitivity." *Optik* 226 (2021): 165842.
- [42] Lee, Seong-Yeon, and Ki-Ju Yee. "Black phosphorus phase retarder based on anisotropic refractive index dispersion." *2D Materials* 9.1 (2021): 015020.
- [43] Yang, Xianchao, et al. "Analysis of graphene-based photonic crystal fiber sensor using birefringence and surface plasmon resonance." *Plasmonics* 12 (2017): 489-496.
- [44] Dash, Jitendra Narayan, Ritwick Das, and Rajan Jha. "AZO coated microchannel incorporated PCF-based SPR sensor: a numerical analysis." *IEEE Photonics Technology Letters* 30.11 (2018): 1032-1035.
- [45] Liu, P. Y., et al. "An optofluidic imaging system to measure the biophysical signature of single waterborne bacteria." *Lab on a Chip* 14.21 (2014): 4237-4243.

- [46] Upadhyay, Anurag, et al. "Analysis of proposed PCF with square air hole for revolutionary high birefringence and nonlinearity." *Photonics and Nanostructures-Fundamentals and Applications* 43 (2021): 100896.

APPENDIX 1: Plagiarism Report



Page 1 of 78 - Cover Page

Submission ID trn:oid::27535:99428142

Plakshi

Plakshi Msc Thesis.docx

 Delhi Technological University

Document Details

Submission ID

trn:oid::27535:99428142

Submission Date

Jun 5, 2025, 9:53 AM GMT+5:30

Download Date

Jun 5, 2025, 11:02 AM GMT+5:30

File Name

Plakshi Msc Thesis.docx

File Size

31.3 MB

72 Pages

14,181 Words

77,817 Characters



Page 1 of 78 - Cover Page

Submission ID trn:oid::27535:99428142

9% Overall Similarity

The combined total of all matches, including overlapping sources, for each database.

Filtered from the Report

- Bibliography
- Quoted Text
- Cited Text
- Small Matches (less than 12 words)

Exclusions

- 2 Excluded Sources

Match Groups

- 71 Not Cited or Quoted 9%**
Matches with neither in-text citation nor quotation marks
- 0 Missing Quotations 0%**
Matches that are still very similar to source material
- 0 Missing Citation 0%**
Matches that have quotation marks, but no in-text citation
- 0 Cited and Quoted 0%**
Matches with in-text citation present, but no quotation marks

Top Sources

- 5% Internet sources
- 6% Publications
- 4% Submitted works (Student Papers)

Integrity Flags

1 Integrity Flag for Review

- Replaced Characters**
5 suspect characters on 7 pages
Letters are swapped with similar characters from another alphabet.

Our system's algorithms look deeply at a document for any inconsistencies that would set it apart from a normal submission. If we notice something strange, we flag it for you to review.

A Flag is not necessarily an indicator of a problem. However, we'd recommend you focus your attention there for further review.



APPENDIX 2: Research Publication-1

Plasmonics
<https://doi.org/10.1007/s11468-024-02723-5>

RESEARCH



Highly Sensitive Black Phosphorus–Layered SPR-PCF Refractometric Sensor

Plakshi Gupta¹ · Akash Khamaru¹ · Ajeet Kumar¹

Received: 7 November 2024 / Accepted: 13 December 2024
© The Author(s), under exclusive licence to Springer Science+Business Media, LLC, part of Springer Nature 2025

Abstract

This work presents a D-shaped surface plasmon resonance (SPR)-based photonic crystal fiber (PCF) sensor with a coating of gold-TiO₂ as a plasmonic material along with black phosphorus (BP) nano-films which works as a sensitivity enhancer functioning in visible to near-infrared spectrum. The affixed BP layers offer a direct bandgap, consequently advancing the proposed sensor's performance. The designed sensor is employed for the detection of a broad range of refractive indices limiting from 1.3–1.4. Various fabrication procedures are discussed for layering of BP films on the PCF surface such as liquid peeling and pulsed laser precipitation technique. Along with the influence of BP layers, the thickness of gold and TiO₂ is also optimized for the extraction of favorable outputs. The dimensions of respective cladding air holes of the PCF are also influenced to assess the effectiveness of the proposed sensor. The dynamic sensitivity of the proposed sensor elevated from 9000 to 23,300 nm/RIU with the incorporation of the BP films in the designed PCF RI detector. Additionally, a high amplitude sensitivity of 7446.56 RIU⁻¹ is also achieved. The theoretical structure is numerically analyzed using the finite element method in COMSOL Multiphysics Software. The extracted enhanced sensitivity perfectly elaborates the efficacy of the BP layers in the PCF-SPR RI sensor and builds our suggested sensor as a prospective participant in modern plasmonic sensors.

Keywords Black phosphorus · D-shaped · Surface plasmons · Wavelength sensitivity · Amplitude sensitivity

Introduction

Surface plasmons (SPs) were initially introduced by Ritchie, in the 1950s [1]. By applying the theory of SPs, the prism-coupled SPR configuration was studied by Otto where prism and plasmonic materials were separated by the dielectric medium [2]. The setup's configuration was then upgraded by the Kretschmann where prism and plasmonic material were in direct contact [3]. The latter configuration was used for generating surface plasmon waves, by matching the frequency of incident light and surface electrons (i.e.,

free electrons in metals). In the 1980s, these methods were used to demonstrate SPR sensors for biological and chemical sensing [4].

Surface plasmon resonance is a phenomenon that occurs at the surfaces of metals (like gold, silver), whenever electrons interact with a light beam that strikes the surface at a particular angle. The interaction is sensitive to the changes in the nearby environment or simply the changes in refractive index. Compared with the traditional sensing methods, the sensing technology adopting the surface plasmon resonance technique has the advantage of real-time analysis; it is much more sensitive to the changes in surroundings and is label-free. Therefore, the SPR sensing approach has proved a remarkable detection technique due to its higher sensitivity and a vast number of applications like biosensing, antibody interaction, clinical trials, food quality analysis, and gas detection. The conventional prism-based Kretschmann setup is being widely used for SPR sensors, in which the prism is coated with the plasmonic material. The deviation in the refractive index changes the propagation constant of the surface plasmon mode. This results in variation in coupling conditions. But the prism-based SPR sensor requires

✉ Ajeet Kumar
ajeetdph@dtu.ac.in
Plakshi Gupta
plakshigupta_23mscphy74@dtu.ac.in
Akash Khamaru
akashkhamaru_23phd02@dtu.ac.in

¹ Advanced Photonics Simulation Research Laboratory,
Department of Applied Physics, Delhi Technological
University, Shahbad Daultpur, Bawana Road, Delhi 110042,
India

APPENDIX 3: Research Publication-2

Plasmonics
https://doi.org/10.1007/s11468-025-02911-x

RESEARCH



Black Phosphorus-Based SPR Photonic Crystal Fiber Biosensor for Urinary Tract Infection Detection

Plakshi Gupta¹ · Akash Khamaru¹ · Ajeet Kumar¹

Received: 18 February 2025 / Accepted: 18 March 2025
© The Author(s), under exclusive licence to Springer Science+Business Media, LLC, part of Springer Nature 2025

Abstract

The presented work focused on a photonic crystal fiber (PCF)-based urinary tract infection (UTI) biosensor operating on the principle of surface plasmon resonance (SPR) combined with black phosphorus (BP) layers as a plasmonic enhancer to increase the sensitivity of the sensor. There are three types of bacteria that can cause UTI: *Pseudomonas*, *Escherichia coli*, and *Enterococcus faecalis*, whose refractive indices are already available in various experimental literatures and having magnitudes 1.371, 1.388, and 1.3921, respectively. The analysis is carry forwarded by applying the finite element method (FEM)-based simulation software-COMSOL Multiphysics. The PCF structure comprises TiO₂, gold, and BP layers, forming a plasmonic layer conjugate along with square air holes running along its length. The analysis also contains the comparison of the sensor's performance with and without incorporating the BP layers, which shows that the wavelength sensitivity increases exponentially. When the sensor is composed without the BP layers, the wavelength sensitivity for different types of bacteria is 2361.11, 2924.52, and 3239.92 nm/RIU, whereas when the BP layers are placed on the top of the gold layer, the wavelength sensitivity goes as high as 5138.88, 7264.15, and 8936.69 nm/RIU. This shows an increase in the sensitivity by much more than 50%, which helps our PCF biosensor stand out as an effective alternative among other designed UTI-focused sensors.

Keywords Urinary Tract Infection · PCF Biosensor · Surface Plasmon Resonance · Black Phosphorus · Wavelength Sensitivity

Introduction

UTI (urinary tract infection) is a bacterial infection that affects kidneys, urethra, ureters, and bladders and affects more than 150 million people worldwide annually. The study of UTI varies with age, gender, abnormalities, pregnancy, anatomic, and many other factors. It mostly affects women than men due to anatomical differences in genitourinary tract [1]. According to studies, 3 to 24% of women are affected with UTI during pregnancies which leads to complications

such as premature birth, anemia, chronic kidney failure, and lesser birth weight of infants. Some of the symptoms of UTIs range from pelvic pain and vomiting to severe complications like multi-organ failure or even deaths. So, timely identification and treatment of UTI is important to reduce maternal morbidity and recurrence.

UTIs can be caused by both gram-positive and gram-negative microorganisms (known as uropathogens), where *Escherichia coli* (*E. coli*) is a gram-negative bacteria. Some other bacteria leading to UTIs are *Enterococcus faecalis* (*E. faecalis*), *Pseudomonas aeruginosa*, *Klebsiella pneumoniae*, and *Staphylococcus saprophyticus* [1]. Generally, conventional methods such as urine culturing, urine microscopy, and other methods like ELISA, PCR, and biosensor detectors are used for UTI detection [2]. Urine culture is the standard method and economically friendly approach for diagnosis of uropathogens but is also time-consuming, labor-intensive, and requires growth media. To overcome these challenges, ELISA and PCR can also be used, which are rapid detection techniques but still require skilled labor and expensive equipment

✉ Ajeet Kumar
ajeetdph@dtu.ac.in

Plakshi Gupta
plakshigupta_23msep74@dtu.ac.in

Akash Khamaru
akashkhamaru_23phdap02@dtu.ac.in

¹ Advanced Photonics Simulation Research Laboratory,
Department of Applied Physics, Delhi Technological
University, Shahbad Daultpur, Bawana Road, Delhi 110042,
India

APPENDIX 4: Conference Certificate

	PIOT-NICS-2024 12 - 15 December
16th International Conference on FIBER OPTICS AND PHOTONICS	
<i>Certificate of Participation</i>	
This is to certify that Prof./ Dr./ Mr./ Miss <u>Ms. Plakshi Gupta</u> from <u>Delhi Technological University</u>	
attended/ presented Paper in the	
16th International Conference on Fiber Optics and Photonics December 12 - 15, 2024, Kalidas Auditorium, IIT Kharagpur, India	
Organized by INDIAN INSTITUTE OF TECHNOLOGY KHARAGPUR	
<u>Sarvag</u> Organizing Secretary	<u>S. K.</u> Co-Convenor and TPC Chair
	<u>S. K.</u> Convener

APPENDIX 5: Proof of SCIE Indexing

The screenshot shows the Clarivate Master Journal List search results for the journal "Plasmonics". The search was performed on the website mjl.clarivate.com/search-results. The user is logged in as Akash Khamaru. The search results show that "Plasmonics" is an exact match found in the Science Citation Index Expanded (SCIE) database. The journal is published by Springer, One New York Plaza, Suite 4600, New York, United States, NY, 10004. The ISSN is 1557-1955 / 1557-1963. The Web of Science Core Collection is Science Citation Index Expanded. The Additional Web of Science Indexes are Current Contents Physical, Chemical & Earth Sciences | Essential Science Indicators. The search results also show that the journal is indexed in the Social Sciences Citation Index (SSCI), Arts & Humanities Citation Index (AHCI), and Emerging Sources Citation Index (ESCI). The search results are sorted by Relevancy. The search results are found on page 1 of 5 results. The search results are shared via a link: [Share These Results](#). The search results are also shared via a link: [Share This Journal](#). The search results are also shared via a link: [View profile page](#). The search results are also shared via a link: [? 5](#).

Clarivate

Welcome, Akash Khamaru

Settings Log Out

Master Journal List Search Journals Match Manuscript Downloads Help Center

Already have a manuscript? Use our Manuscript Matcher to find the best relevant journals! Find a Match

Refine Your Search Results

Plasmonics Search Sort By: Relevancy

Active Filters

SCIENCE CITATION INDEX EXPANDED (SCIE) SOCIAL SCIENCES CITATION INDEX (SSCI) ARTS & HUMANITIES CITATION INDEX (AHCI) EMERGING SOURCES CITATION INDEX (ESCI)

Search Results

Found 5 results (Page 1) Share These Results

Exact Match Found

PLASMONICS

Publisher: SPRINGER, ONE NEW YORK PLAZA, SUITE 4600, NEW YORK, United States, NY, 10004

ISSN / eISSN: 1557-1955 / 1557-1963

Web of Science Core Collection: Science Citation Index Expanded

Additional Web of Science Indexes: Current Contents Physical, Chemical & Earth Sciences | Essential Science Indicators

Share This Journal View profile page ? 5

Nifty bank +0.25%

Search

ENG IN 10:20:12 05-06-2025